The High-Luminosity upgrade of the LHC: Physics and Technology Challenges for the Accelerator and the Experiments

2016 J. Phys.: Conf. Ser. 706 022002

(http://iopscience.iop.org/1742-6596/706/2/022002)

Journal of Physics: Conference Series **706** (2016) 022002 doi:10.1088/1742-6596/706/2/022002

The High-Luminosity upgrade of the LHC

Physics and Technology Challenges for the Accelerator and the Experiments

Burkhard Schmidt, CERN October 2015

Abstract

In the second phase of the LHC physics program, the accelerator will provide an additional integrated luminosity of about 2500/fb over 10 years of operation to the general purpose detectors ATLAS and CMS. This will substantially enlarge the mass reach in the search for new particles and will also greatly extend the potential to study the properties of the Higgs boson discovered at the LHC in 2012. In order to meet the experimental challenges of unprecedented *pp* luminosity, the experiments will need to address the aging of the present detectors and to improve the ability to isolate and precisely measure the products of the most interesting collisions. The lectures gave an overview of the physics motivation and described the conceptual designs and the expected performance of the upgrades of the four major experiments, ALICE, ATLAS, CMS and LHCb, along with the plans to develop the appropriate experimental techniques and a brief overview of the accelerator upgrade. Only some key points of the upgrade program of the four major experiments are discussed in this report; more information can be found in the references given at the end.

1. Physics Motivation for the High Luminosity LHC

The Physics Program at the Large Hadron Collider (LHC) had a remarkable start. In the first physics run in 2011 and 2012, the collider reached a peak luminosity of 7.7 x 10^{33}/cm^2/s, more than 75% of its design luminosity, and delivered an integrated luminosity of about 25/fb to each of its two general purpose experiments, ATLAS and CMS, and smaller data sets to LHCb and ALICE. This data has yielded a vast quantity of physics results, summarized in about 1000 publications in referred journals so far. One of highlights has been the observation in 2012 of a new particle of mass 125 GeV by the ATLAS and CMS collaborations [1, 2]. This particle was identified as the Standard model (SM) Higgs Boson. Figure 1 shows the results from ATLAS and CMS that contributed to establishing the existence of this new particle.

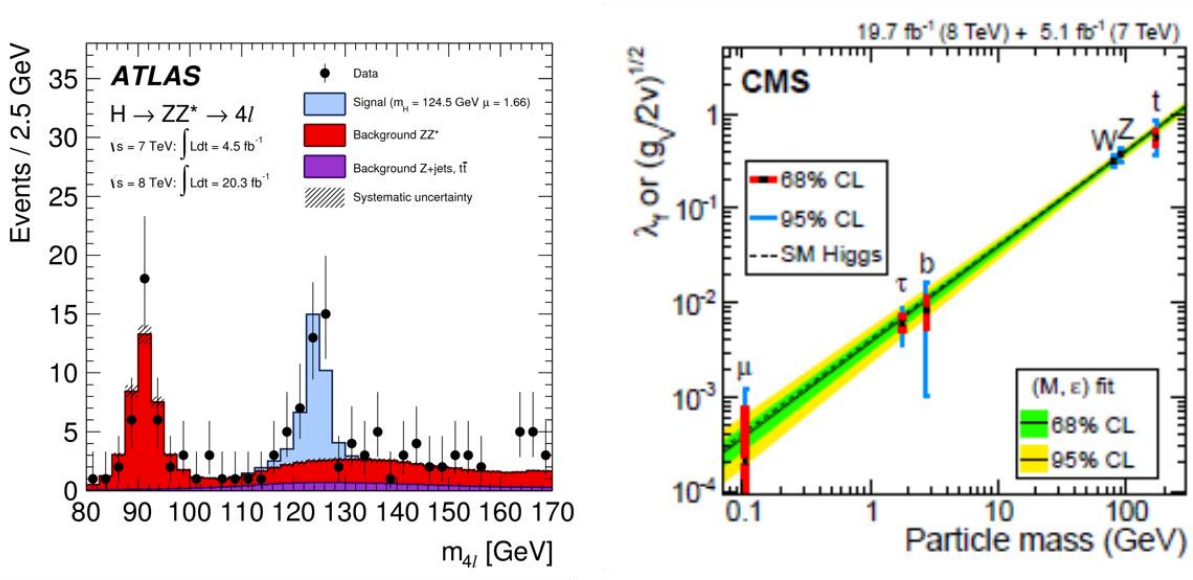

Figure 1: Left: The Higgs to 4 lepton mass spectrum of ATLAS with a peak near 125 GeV. Right: The Observed precision on the Higgs boson couplings as a function of boson or fermion masses, as determined by CMS.

In addition to discovering the new boson, ATLAS and CMS were able to begin the detailed study of its properties to show that it was indeed a Higgs boson. The decays of the new boson to the gauge bosons of the SM, the *W, Z,* and the photon, were established, each with more than 5 standard deviation significance. By using a combination of theory predictions for the decays and production, the couplings of the new boson to these particles have been determined and are shown in Figure 1 as well. They follow the mass dependence uniquely characteristic of the Higgs field. Moreover, searches for the decay to fermions such as $\tau^+\tau^-$ are at the edge of significance and their corresponding couplings are consistent with SM expectations for the Higgs. Studies of the properties of Higgs decay have provided compelling evidence that the spin and parity of the new boson are indeed 0^+.

Another striking result from Run I has been the observation of the very rare decay $B_s^0 \rightarrow \mu^+\mu^-$ through a combined analysis of CMS and LHCb data [3]. The signal is shown in Fig. 2. This decay is very highly suppressed in the SM, but the decay rate is theoretically well-predicted. If new physics is present it might either enhance or suppresses the decay rate. The observed branching ratio is $3.0\ ^{+1.0}_{-0.9} \times 10^{-9}$, consistent with the expectations of the SM. This result places very strict constraints on models of new physics. The companion decay, $B^0 \rightarrow \mu^+\mu^-$, is predicted to have a branching fraction that is a factor of 20 lower than the B_s. Improving the precision of the B_s^0 measurement and observing the B^0 decay and measuring its branching fraction are important goals for the HL-LHC, as further discussed in section 4.1.

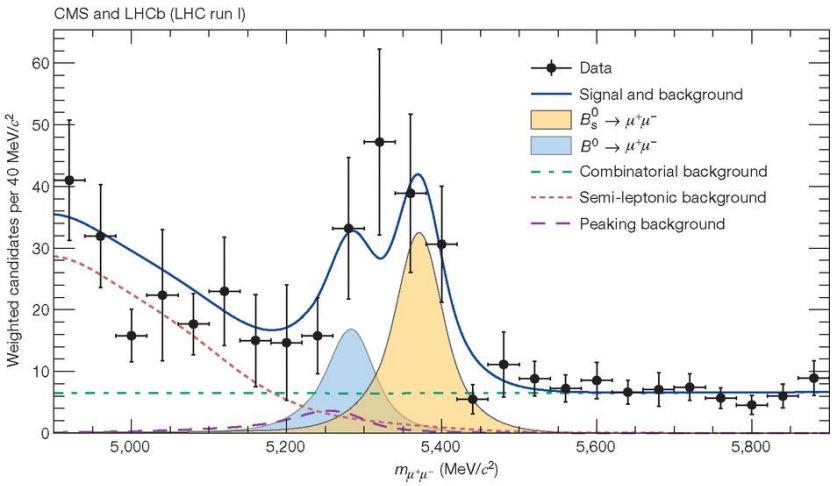

Figure 2: Weighted distribution of the di-muon invariant mass, $\mu^+\mu^-$. Superimposed on the data points in black are the combined fit (solid blue line) and its components: the B_s^0 (orange shaded area) and B^0 (blue shaded area) signal components; the combinatorial background (dash-dotted green line); the sum of the semi-leptonic backgrounds (dotted salmon line); and the peaking backgrounds (dashed violet line). The horizontal bar on each histogram point denotes the size of the binning, while the vertical bar denotes the 68% confidence interval.

1.1 Higgs boson precision measurements

An important component of the HL-LHC programme is to carry out studies involving the recently discovered 125 GeV Higgs boson. One aspect is precision measurements of the properties of this scalar particle, in order to test the Standard Model pattern of couplings to elementary particles. Additionally, because of the hierarchy problem with quantum instability of the Higgs sector, many models of new physics affect precision Higgs observables, even in cases where the corresponding new particles are hard to discover experimentally. The ATLAS and CMS experiments expect comparable precision, with an estimated uncertainty of 2-5% for many of the investigated Higgs boson couplings to elementary fermions and bosons, demonstrating that with an integrated luminosity of 3000 fb-1 the HL-LHC is a very capable precision Higgs physics facility. Figure 3 illustrates the improvements in coupling measurements expected for weak bosons and fermions with 3000/fb of data.

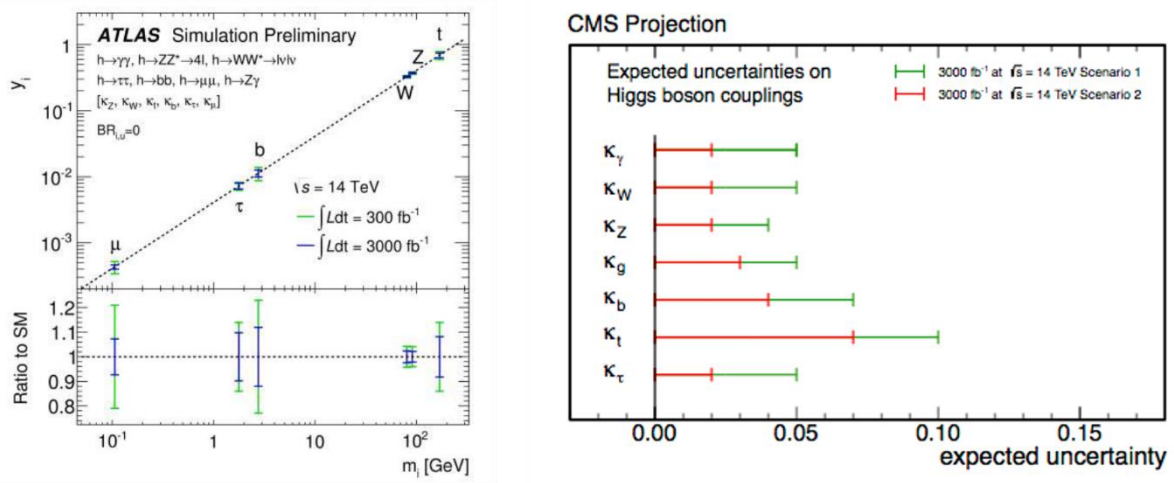

Figure 3: Left: Projected results of ATLAS for the reduced coupling scale factors for weak bosons and fermions as a function of the particle mass, assuming a data set of 300/fb or 3000/fb and a SM Higgs boson with a mass of 125 GeV. Right: CMS projection for the expected uncertainties n Higgs boson couplings. Scenario 1 assumes that the systematic uncertainties are as today, Scenario 2 that the experimental uncertainties scale as 1/√L and the theoretical uncertainties half.

Along with improving the precision of Higgs-sector measurements, the substantial luminosity of HL-LHC will make it possible to probe important rare processes involving the Higgs boson. Some examples involve rare decays, such as $H \rightarrow Z\gamma$, or those involving second generation fermion couplings, which can open a novel window on the problem of flavour. Off-shell and high transverse momentum Higgs production allows access to new physics near the TeV scale that may otherwise be hidden, only partially overlapping with the sensitivity to BSM (and SM) physics coming from precision Higgs measurements and providing complementary information (for details see [4+5] and ref. therein).

Finally, the HL-LHC may have the potential to study di-Higgs production. In the Standard Model, with the Higgs boson mass and the Higgs-field (ϕ) vacuum expectation value now both known, the structure of the Higgs potential is fully predicted. This is because the potential involves just two terms, proportional to ϕ^2 and ϕ^4. An elementary field potential of this kind has never been seen before in nature and it is crucial to test whether it is indeed the potential associated with the actual vacuum. A study of the Higgs boson self-coupling provides one such test, because the self-coupling is related to the third derivative of the Higgs potential at its minimum, uniquely predicted in the Standard Model. One main avenue for studying the self-coupling is through di-Higgs production, which is sensitive to the (off-shell) $H^* \rightarrow HH$ process. It should be noted, however, that this interferes with other mechanisms for the production of two Higgs bosons, which complicates the determination of the self-coupling. Furthermore, new-physics can modify the relation between the Higgs potential and di-Higgs production; for example di-Higgs production can be greatly enhanced in cases where the Higgs is composite rather than elementary.

1.2 Search for signatures of physics beyond the Standard Model

The SM describes an impressive variety of experimental data over a very large energy range. Nonetheless, for numerous reasons (e.g. the absence of a description of the gravitational interaction), it is postulated that the SM may be a low energy effective theory. Furthermore, the SM does not provide answers several of the fundamental questions in particle physics including:

- What is the nature of the dark matter we observe in the Universe?
- Are the fundamental forces unified?
- How does QCD behave under extreme conditions?
- Do matter and antimatter properties differ?

The answer to most of them require new physics. In fact, the one particular important shortcoming of the SM given the recent discovery of a relatively low mass Higgs boson is that the mass of a scalar particle such as the Higgs receives large radiative corrections, on the order of M_{Planck}. One of the most pressing questions in particle physics is therefore, whether or not there exists new particles around the TeV scale which stabilise the Higgs mass and cancel the quadratic divergences in the Higgs sector. One of the favoured model is Supersymmetry (SUSY). SUSY is a hypothetical new symmetry of nature which relates fermions and bosons and suggest partner particles, called sparticles. The cross sections for strongly produced sparticles are relatively large, cross sections for electroweak particles like neutralinos and charginos are several orders of magnitude smaller and thereby benefit significantly from the large integrated luminosity provided by the HL-LHC.

1.2.1 Search for neutralinos and charginos

One of the processes with a low production cross section, and therefore strongly dependent on high luminosity, is the direct production of the supersymmetric partners of the electroweak gauge bosons. The SUSY partner of the Higgs particle, the higgsino, is bound by the Higgs mass parameter μ to be close to the Higgs mass. The higgsino mixes with the partner particles of the other bosons to mass eigenstates, called neutralinos (χ^0) and charginos ($\chi^{\pm}$). At least a few of these particles are expected to be light (of the order of several hundred GeV) in natural supersymmetry.

Weak gauginos can originate in cascade decays from squark and gluino production or can be directly produced via weak interactions. In scenarios with heavy gluinos and squarks, the direct pair production of weak gauginos can become the dominant SUSY process at the LHC. The decays of neutralinos and charginos, as illustrated in Fig. 4, can lead to clean final states with three leptons and missing transverse momentum. The χ_1^0 is in this model the lightest SUSY particle (LSP), which is stable, and a viable dark matter candidate. The search for direct production of $\chi_1^{\pm}$ and χ_2^0 with decays as illustrated in Fig. 7 and interpreted in the context of a simplified SUSY model where a branching ratio via W and Z^0 bosons of 100% is assumed. Nature might well have a lower BR and several other decays, which are then expected to become observable. With an integrated luminosity of 3000/fb neutralinos χ_2^0 and charginos $\chi_1^{\pm}$ up to a mass of 700 GeV for χ_1^0 masses of up to 200 GeV can be discovered with a significance of 5σ, as shown in Fig. 4 (right).

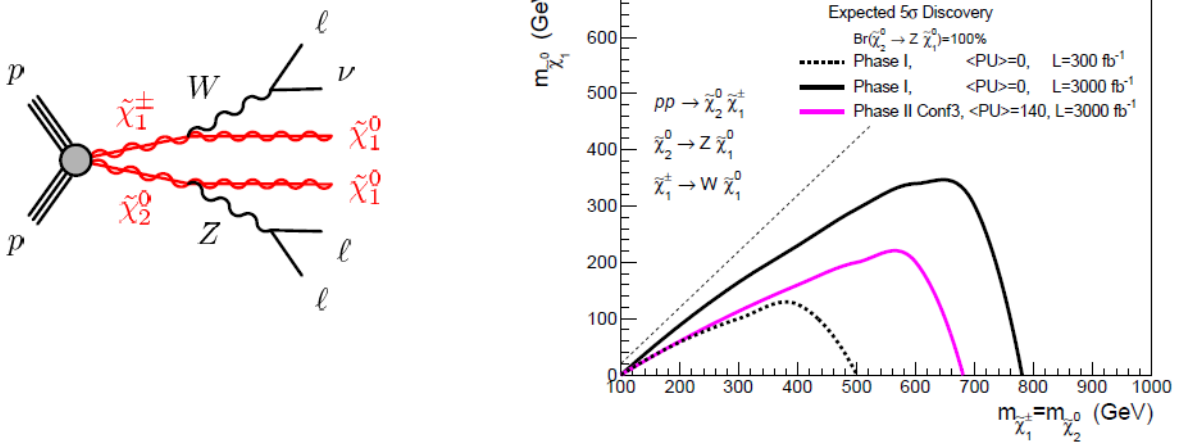

Figure 4: Left: The Feynman diagram for the χ_2^0 and $\chi_1^{\pm}$ simplified model. Right: Projections of the discovery reach for electroweak production of χ_2^0 and $\chi_1^{\pm}$ that decay via W and Z bosons into χ_1^0. The magenta curve is the realistic reach obtainable under HL-LHC luminosity conditions. This can be compared with the black solid curve that shows what the reach would be if there were no pileup effects, or equivalently pileup effects were completely mitigated. This curve in turn can be compared with the black dashed curve in order to see the increase in reach due to the luminosity provided by the HL-LHC with respect to LHC.

1.2.2 Direct stop production

Naturalness arguments suggest the light top squark mass eigenstate to be below 1-1.5 TeV. While stops are the lightest coloured SUSY particles, the cross section for direct stop pair production is only about 1 fb for 1.5 TeV. Such searches are therefore expected to benefit from the large luminosity of the HL-LHC and are studied in this section.

Stops can decay in a variety of modes which are very much dependent on the parameters of the SUSY model assumed. Typically, SUSY final state events contain top or b-quarks, *W/Z* or Higgs bosons, and an LSP. Pair production signatures are thus characterized by the presence of several jets, including *b*-jets, large missing transverse momentum and possibly leptons. In some cases the dominant decay chains will be difficult to separate from the SM background and dedicated analyses must be employed. For the discovery of such scenarios high luminosity is a key factor.

The search presented here aims for the discovery of pair-produced stops that are assumed to decay to a top quark and the LSP ( ), as shown in Fig. 5 (left). Here it is required that the produced top quark is on shell, m(t̃) – m (χ_1^0) > m(t). The final state for such a signal is characterized by a top quark pair produced in association with large missing transverse momentum from the undetected LSPs. Two studies are carried out as counting experiments targeting the scenario described above, a zero lepton selection requiring jets, b-jets and a large missing transverse momentum and a one lepton selection with stringent requirements on missing transverse momentum. For the calculation of the discovery reach, shown in Fig. 5 (right), the zero lepton and one lepton channels are statistically combined.

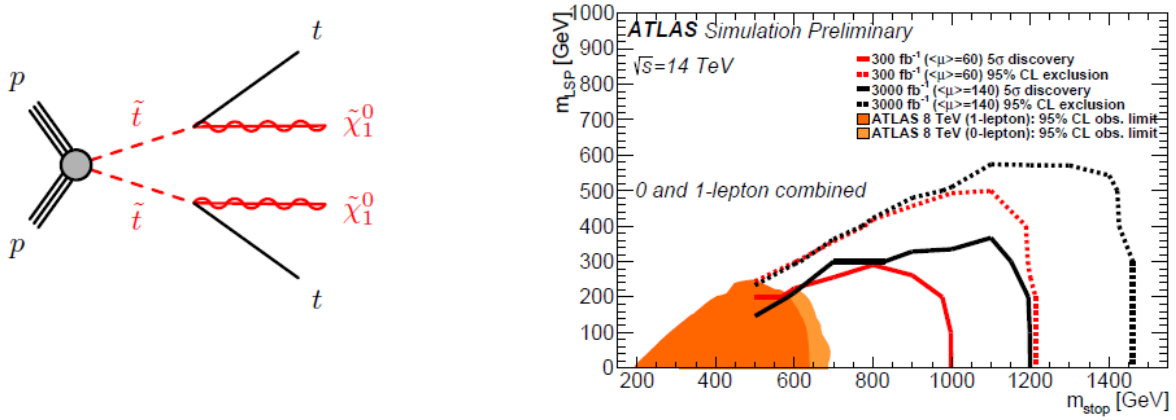

Figure 5: Left: The Feynman diagram for the simplified model of direct stop production. Right: The 5σ discovery reach (b) for 300 fb1 (solid red lines) and for 3000 fb1 (solid black line). The corresponding 95% exclusion limits are shown as dashed lines.

2. Overview of the High-Luminosity upgrade of the LHC

After 2020, the statistical gain in running the accelerator without a considerable luminosity increase beyond its design value will become marginal. The running time necessary to half the statistical error in the measurements will be more than ten years at the end of 2019. Therefore to maintain scientific progress and to explore its full capacity, the LHC will need to have a decisive increase of its luminosity. That is why, when the CERN Council adopted the European Strategy for Particle Physics in Brussels on 30 May 2013, its first priority was agreed to be *"[…] the exploitation of the full potential of the LHC, including the high-luminosity upgrade of the machine and detectors with a view to collecting ten times more data than in the initial design, by around 2030 […]"*.

In order to minimize the machine downtimes and maximize the productive use of the LHC for physics, the replacement of the inner triplet magnets (the one responsible to squeeze the beam at collision)

and of all hardware changes needed to enable an ambitious luminosity upgrade will take place in parallel during one shutdown, at around 2023-25 (Long shutdown 3), with some of the modification anticipated in 2019-2020 (LS2). This new phase of the LHC life has been named as High Luminosity LHC (HL-LHC) and has the scope of attaining the astonishing threshold of 3000 fb^{-1} in 10-12 years. All the hadron colliders in the world have so far produced a total integrated luminosity of about 10 fb^{-1}, while the LHC will deliver about 300 fb^{-1} in its first 10-12 years of life.

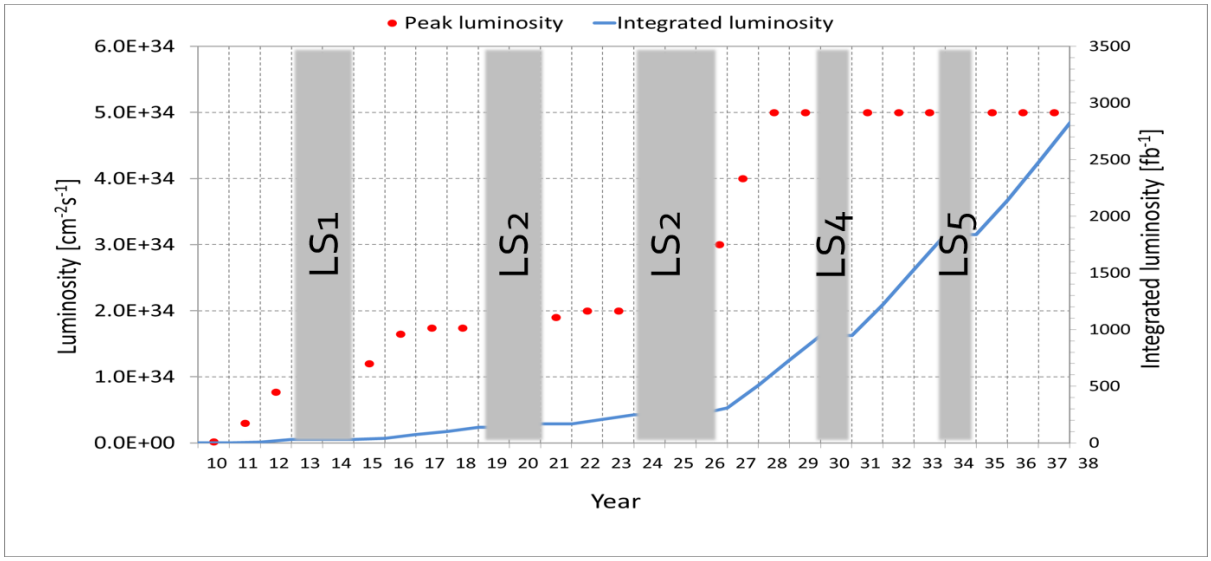

Figure 6: Projected LHC performance through 2038, showing preliminary dates for long shutdowns (LS) of the LHC and projected luminosities.

A new scheme to form the bunch trains in the Proton Synchrotron (PS) will allow the luminosity to exceed the original design before the second long shutdown, LS2, planned for 2019-2020. In LS2, the injector chain will be further improved and upgraded to deliver very bright bunches (high intensity and low emittance). It is anticipated that the peak luminosity could reach 2 x $10^{34}/cm^2/s$ in this first phase of the LHC program, providing an integrated luminosity of over 300/fb by 2023. By 2023, the quadrupoles that focus the beams at the ATLAS and CMS collision regions are expected to be close to the end of their lives due to radiation exposure. There will be another long shutdown, LS3, to replace them with new low-*b* quadrupole triplets. In addition, crab-cavities will be added to optimize the bunch overlap at the interaction region. These changes will produce a significant increase in the LHC luminosity.

The proposed operating scenario is to level the instantaneous luminosity at 5 x $10^{34}/cm^2/s$ from a potential peak value of 2 x $10^{35}/cm^2/s$ at the beginning of fills, and to deliver 250/fb per year for a further 10 years of operation. The schedule of beam operations and long shutdowns, together with projections of the peak and integrated luminosities, is shown in Fig. 6 and is, of course, subject to change.

2.1 HL-LHC upgrade parameters

After collision energy luminosity is the most important parameter of a collider, because it is proportional to the number of useful events.

The instantaneous luminosity *L* can expressed as : $L = \gamma \frac{n_b N^2 f_{rev}}{4\pi \beta^* \varepsilon_n} R; \qquad R = 1/\sqrt{1 + \frac{\theta_c \sigma_z}{2\sigma}}$,

where γ is the proton beam energy in unit of rest mass ; nb is the number of bunches in the machine: 1380 for 50 ns spacing and 2808 for 25 ns ; N is the bunch population, N nominal 25 ns = 1.15×1011 p; frev is the revolution frequency (11.2 kHz) ; β^* is the beam beta function (focal length) at the

collision point (nominal design 0.55 m) ; εn is the transverse normalized emittance (nominal design: 3.75 μm); R is a luminosity geometrical reduction factor (0.85 at 0.55 m of β^*, down to 0.5 at 0.25 m); θc is the full crossing angle between colliding beam (285 μrad as nominal design) ; σ and σz are the transverse and longitudinal r.m.s. size, respectively (16.7 μm and 7.55 cm).

Although the 25ns bunch spacing remains the baseline, given the experience of the first years of operation, 50ns is kept as a viable alternative, in case the e-cloud or other unforeseen effects undermine the 25ns performance. However, the companion LHC detector upgrade project is designing for an average pile up around 140; for 25 ns spacing this means about $5 \cdot 10^{34}$ of luminosity, while at 50ns this means limiting the levelling luminosity to half, if the pile up has to be the same. This translates into a longer run time for the 50ns and inevitably for a request of even higher efficiency, unless higher pile up can be accepted (new concepts like pile density per volume are being explored to overcome absolute pile limitation). Experience with LHC shows that the best set of parameters for actual operation is difficult to predict. An upgrade should provide the potentiality of performance over a wide range of parameters, and eventually the machine and experiments will find the practical best set of parameters in actual operations.

A classical route to the luminosity upgrade is to reduce β^* by means of stronger and larger aperture low-β triplet quadrupoles. With respect to reducing the emittance, this is a local action, rather than a modification of the whole machine and injector chain. The drawback of very small β^* is that it requires larger crossing angle, which entails a reduction of the R geometrical factor, see luminosity expression. In Fig. 7 the reduction factor is plotted vs. β^* values. The most efficient and elegant solution for compensating the geometric reduction factor is the use of so-called 'Crab Cavities'. Special RF 'crab' cavities are capable to generate transverse electric field are used to give a torque to the beam. In this way the beams do not suffer from overlap reduction due to θ_c , as shown in Fig. 7: a crab cavity just rotates each bunch by $\theta_c/2$, such as they collides head on, overlapping perfectly at the collision point. In this way the crossing angle is maintained over the long drift space in the common vacuum beam pipe avoiding the long range beam-beam interactions, but the geometrical reduction is totally suppressed. Of course the same opposite kick must be given to the beam at the opposite side of the collision point. Crab cavities have been successfully tested for the first time in the e^+e^- ring Belle at KEK, however their feasibility for hadron beam has still to be demonstrated.

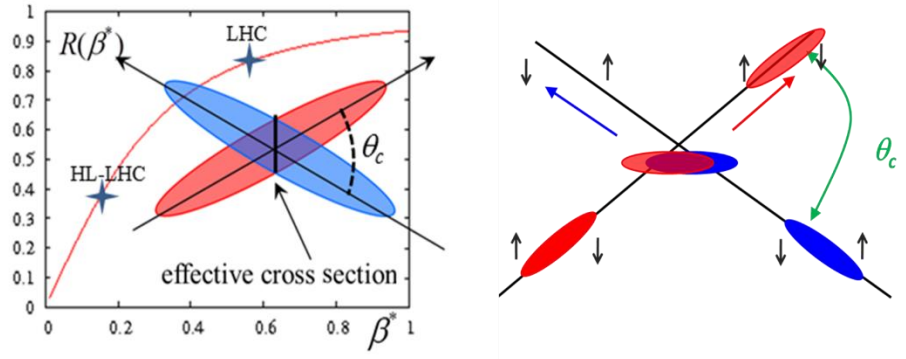

Figure 7: Left: Effect of geometrical reduction factor on luminosity vs. β^* with two operating points shown: nominal LHC and HL-LHC. The sketch of bunch crossing shows the reduction mechanism. Right: Effect of the crab cavity on the beam (small arrows indicate the torque on the beam by transverse varying RF field).

In Table 1 are listed the main parameters for the LHC upgrade in luminosity. For convenience, first are listed the nominal LHC operating parameters, then the upgrade parameters both for 25 ns and for 50 ns bunch spacing. As mentioned 25 ns is our operation target, the 50 ns being a fall-back solution. For both bunch spacing we quote two lists: baseline and stretched parameters, these last being the most ambitious objectives that might enable 300 fb^{-1} per year. The efficiency (last line) is quoted for a goal of 250 fb^{-1}/y. The efficiency of LHC in 2012 after the initial period was above 40%, so the efficiency

proposed for the 25ns is reasonable, nevertheless a big leap forward is required on increasing availability and turnaround time (time from end of physics to next start of physics).

Table 1 : parameters for HL-LHC compared with LHC nominal (in bold the most critical ones).

Parameter	**Nom.** 25 ns	**Stretched** 25 ns	**Stretched** 50 ns	**Baseline** 25 ns	**Baseline** 50 ns
N_b [10^{11}]	1.15	**2.2**	**3.5**	**2.0**	**3.3**
n_b	2808	2808	1404	2808	1404
I [A]	0.56	**1.12**	0.89	**1.02**	0.84
θc [μrad]	300	590	590	590	590
β^* [m]	0.55	**0.15**	**0.15**	**0.15**	**0.15**
ε_n [μm]	3.75	**2.5**	**3.0**	**2.5**	**3.0**
R red.fact.	0.81	0.31	0.33	0.31	0.33
L_{peak} (no crab)	1	7.4	8.5	5.3	7.6
Crabbing	no	**yes**	**yes**	**yes**	**yes**
$L_{peak\ virtual}$	1	24	26	20	23
Lumi level	=	5	2.5	5	2.5
Pileup $L_{lev}=5L_0$	19(27)	140	140	140	140
Eff.†150 days	=	0.59	**0.98**	0.63	**1.0**

For physics purposes, luminosity integrated over time is the relevant parameter: however integrated luminosity does not depend on collider performance only, but also on many external parameters (injector performance, availability and quality of technical services, etc.). The expectations in term of integrated luminosity of Fig. 8 are based on LHC capability and general run parameters (peak luminosity, burning rate of protons, duration of a run, etc.) and on the running experience at CERN, which includes the external factors previously mentioned.

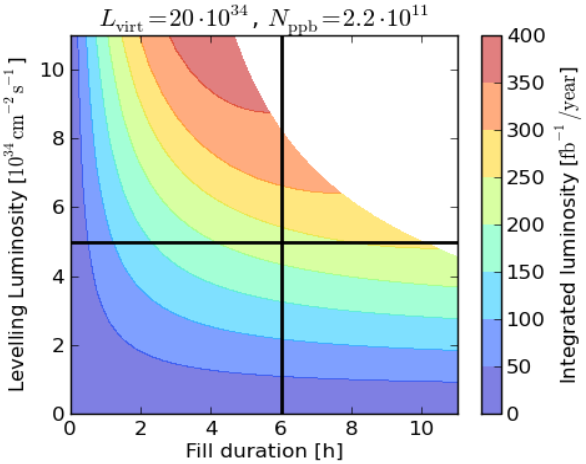

Figure 8: Theoretical LHC performance calculated by assuming 160 days of *pp* physics with an efficiency factor of 50 %, 3h of turnaround time, including the burn-off decay of the luminosity assuming the peak virtual luminosity and initial bunch population considered for the HL-LHC. The white area is the region for which it would be more efficient to restart a fresh fill and therefore the performance is not evaluated. The black lines highlight the average fill duration of the 2012 LHC run and the baseline maximum instantaneous luminosity tolerated by the ATLAS and CMS experiments.

2.2. Hardware modifications and challenges of HL-LHC

While the LHC has been the summit of 30 years of hadron collider evolution, its high luminosity upgrade will open the gate for new technologies and new concepts that will likely mark the next generation of colliders, either for hadrons or for leptons. The total hardware renovation and upgrade of LHC are equivalent to manufacturing and installing about 1.2 km of a new accelerator, in various places of the LHC ring, as shown in Fig. 9, which indicates the extend of the challenge.

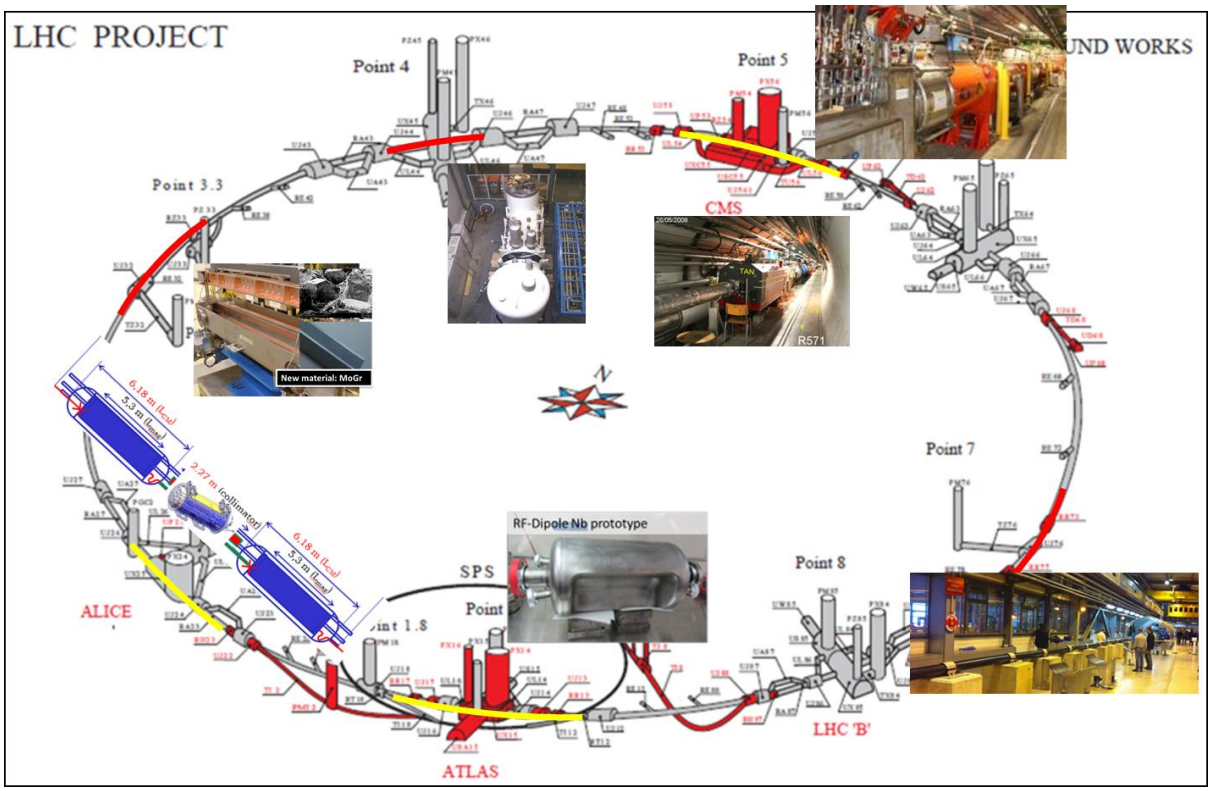

Figure 9: LHC ring areas where major works are required for the upgrade are marked with solid line. In yellow when works concern insertion regions (IRs) with experiments and in red when works concern IRs with only machine functions (length of solid lines not to scale).

A detailed summary of the accelerator upgrade is given in Ref. [6]. In the following only two aspects are briefly discussed, the magnets in the interaction regions and matching sections, and the crab cavities.

2.2.1 Magnets in the interaction regions and matching sections

The present LHC constitutes the summit of 30 years of development in the domain of superconducting technologies: Nb-Ti based magnets are pushed to their limits: very compact two-in-one magnets provide 8.3 T operating field by using superfluid helium cooling (magnets are designed, and many have been tested, up to 9 T). Figure 10 illustrates the progress over the years from the resistive magnet era. The upgrade heavily relies on the success of the advanced Nb_3Sn technology, since Nb-Ti superconductor cannot go beyond 9 T. Nb_3Sn has been under development for more than ten years and has now reached a maturity that allows designs of real equipment based on it. Nb_3Sn has been used in solenoids for NMR spectroscopy for more than 20 years. Nb_3Sn has also a higher temperature margin than Nb-Ti, therefore making easier dealing with heat deposition issue. The field quality is still a factor two worse than Nb-Ti but is steadily improving: last prototypes have, nearly, collider quality. The cost of the superconductor remains much higher than Nb-Ti but the total cost of the system, also considering a less demanding cryogenics, is only about 50% higher.

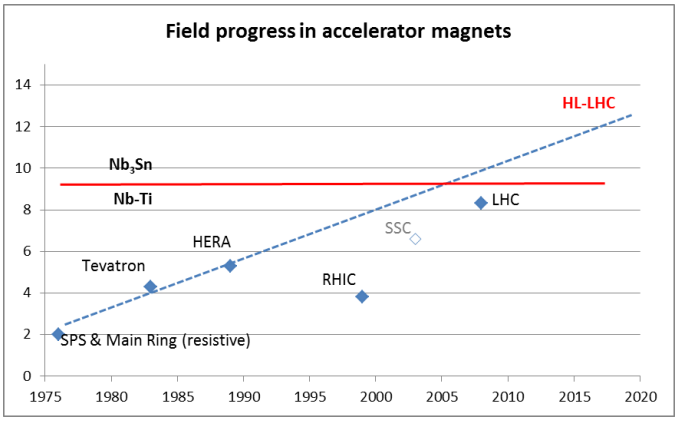

Figure 10: Progress of accelerator magnets for hadron colliders: from 2 to 9 Tesla is the realm of Nb-Ti; beyond 9 Tesla, Nb_3Sn is needed.

2.2.2 Crab cavities

Superconducting (SC) RF cavities of large sizes (with f = 400 MHz), and based on Nb coated Cu technology developed for LEP, are employed in the LHC. The Crab Cavities for LHC will go beyond the state-of-the art for two reasons. The first is that the transverse cavity dimensions are limited by the 194 mm distance of the second beam, a value smaller that λ/4 of 400 MHz wave, practically excluding the well-known geometry of an elliptical cavity: this calls for an unconventional, compact design. The second reason is the demand for very exact control of the phase of the RF (to better than 0.001°), since the slightest phase error would not only offset the bunch head and tail as required for head-on collisions with a non-zero crossing angle, but also the centre of the bunches, which for the very small transverse size of the bunches would lead to an offset of the entire bunch and thus to a significant luminosity loss. For the accelerating cavities, a special region around Point 4 was created, see Fig. 7, in which the beam separation is increased, by the use of magnetic doglegs, to 400 mm in order to allow the installation of the elliptical 400 MHz accelerating cavities. Compact Crab Cavities could be installed on either side of each high luminosity Points 1 and 5, without additional doglegs, but their design would definitely be beyond the present state-of-the-art of SCRF cavity design. The challenging requirement to the precise phase control is equally beyond the state-of-the-art, but similar requirements are found in modern XFEL light sources and in next generation linear colliders. Of large concern are the failure modes of the Crab Cavities, which must be studied in detail in order to allow safe operation of the machine. As mitigation scheme, would the crab cavity not be usable in LHC, is to collide flat beams at the smallest possible crossing angle, by pushing the compensating wires for the long range beam-beam interactions.

3. Performance requirements and the upgrades of ATLAS and CMS

The basic goal of the upgrades of ATLAS and CMS is to maintain the excellent performance of the detectors in terms of efficiency, resolution, and background rejection for all the physics objects used in the analysis of the data. The main challenges that must be overcome to achieve this goal are radiation damage to the detectors from the high integrated luminosity of the HL-LHC and the very high “pileup” that comes from the high instantaneous luminosity. In this section, each of these challenges is described in general terms.

3.1 Radiation damage to the experiments at the HL-LHC

The LHC will produce collisions at a rate of about 5 x 10^9/s. The particles emerging from these collisions and the radioactivity they induce in the material of the detectors and the on-board electronics will cause significant damage and could result in a progressive degradation of the detector performance.

Maintaining the detector performance in the harsh conditions of the LHC was a major consideration in the initial design of the ATLAS and CMS experiments. Considering that the annual dose delivered to the detector per year in the HL-LHC era will be similar to the total dose of all operations from the beginning of the LHC program to the start of LS3, the magnitude of the problem becomes clear. The main source of radiation is from the particles produced in the *pp* collisions. The charged particles, mainly pions, produce ionization in the detectors they pass through. They also undergo nuclear interactions that produce cascades of particles that add to the radiation load. Photons, mainly from π^0 decays, interact in the material of the beam pipe or tracking systems to form e^+e^- pairs or reach the calorimeters where they produce electromagnetic cascades. Particles are also backscattered from the calorimeters or escape from cascades within them. These particles spread out and interact with other detector components. Neutrons, in particular, may travel long distances, slowing down and scattering many times in the detectors, which are largely hermetic. When the neutrons interact, they can also produce photons and electrons. This results in a mixed field of very low energy neutrons, photons, and electrons that have lost any correlation with the bunch structure of the original collisions and form a relatively uniform background in space and time within the detector volume. Simulations are used to predict the magnitude and composition of radiation as a function of luminosity. An example of the predictions of expected radiation levels for HL-LHC conditions in the CMS detector is given in Figure 11, which shows the distribution of absorbed dose over the CMS detector for an integrated luminosity of 3000/fb.

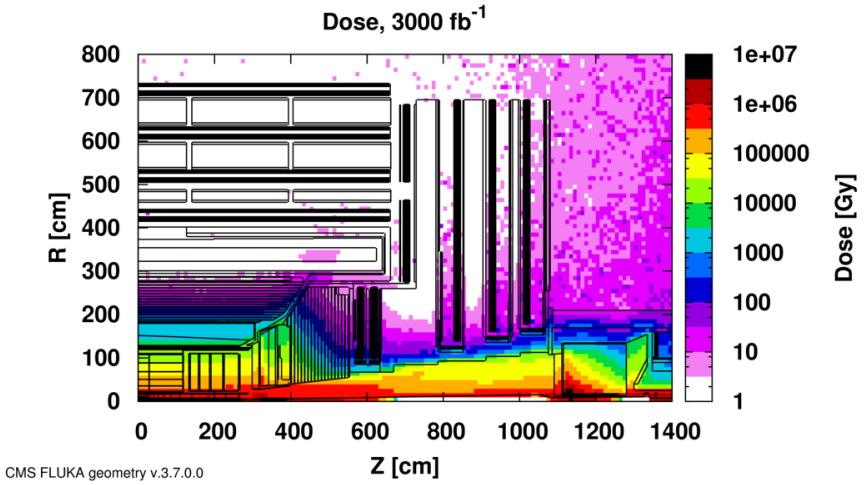

Figure 11: Absorbed dose in the CMS cavern after an integrated luminosity of 3000/fb. R is the transverse distance from the beamline and Z is the distance along the beamline from the Interaction Point at Z=0.

The damage produced in the detectors by this radiation varies from sub-detector to sub-detector. For silicon detectors, radiation produces defects in the silicon lattice that change the bulk electrical properties of the silicon. One consequence is that leakage currents will increase. Trapping centres for charge carriers reduce the Charge Collection Efficiency (CCE), which in turn lowers the signals from charged particles. The full depletion voltage (the voltage required to make the full thickness of the detector depleted from charges, hence making it fully sensitive to a crossing ionizing particle) increases, eventually reaching unsustainable levels and forcing operation with only partial depletion, resulting in lower signals. At the HL-LHC, some detectors will be subjected to fluences as high as 10^{16} particles/cm^2, which will make efficient operation difficult. For calorimeters, which in CMS are mainly scintillating PbWO4 crystals or plastic scintillating tiles with wavelength-shifting fibers embedded in them, the main problem is the loss of transmission of the media through which the scintillation light or wavelength-shifted light must pass. The actual scintillation method does not appear to be harmed by the radiation. This results in a reduction in the signal that can be quite large, in some cases more than 90%, and a corresponding reduction in the resolution. Strategies for mitigating the effects of radiation vary from sub-detector to sub-detector.

3.2 High pileup

Under the foreseen luminosities at the HL-LHC the event pileup (PU) will rise substantially to become a major challenge for the experiments. Each of the colliding beams at the LHC consists of many intense "bunches" of protons. Each bunch has a length with rms of ~5 cm, transverse dimensions of about 10 microns, and contains a few 10^{11} protons. Bunches will be separated in time by 25ns, corresponding to a spatial separation of approximately 750 cm. There are about 2700 filled bunches in each beam and this number cannot be substantially increased. The collision of two bunches is called a "bunch crossing" or "BX" and these occur at a rate of 40MHz. At the nominal luminosity of the HL-LHC, the average number of interactions in a single crossing is approximately 140. Most of these interactions are "soft" or "peripheral" collisions that, if not well understood, are at least well-characterized and do not contribute to the search for new physics at the 0.1-few TeV scale. A relatively small fraction of all collisions are "hard" collisions that contain high transverse momentum particles that may come from new high mass objects. Nevertheless, the presence of some tracks and energy from 140 (on average) extra collisions can confuse or degrade the triggers and the offline reconstruction of the hard scatter.

Since the number of bunches cannot be increased, luminosity increases at the LHC result in higher pileup. Pileup produces many more hits in the tracking detectors, leading to mismeasured or misidentified tracks. It also adds extra energy to the calorimeter measurements, such as jet energies, associated with the collision that contained a hard scatter. Electroweak phenomena, which are of special interest, are often characterized by having "isolated" leptons, that is leptons or photons with very little activity around them. Energy or tracks from pileup can contribute to an activity that is not due to the collision containing the leptons or photons and cause them to appear non-isolated. Pileup confuses the trigger and also the offline reconstruction and interpretation of events. It increases the amount of data that has to be read out in each BX that contains a hard scatter. In fact, at the HL-LHC, most of the data read out will be associated with the "pile-up" collisions rather than the collision containing hard scatters. It also increases the execution time for the reconstruction of events in the High Level Trigger and the offline analysis.

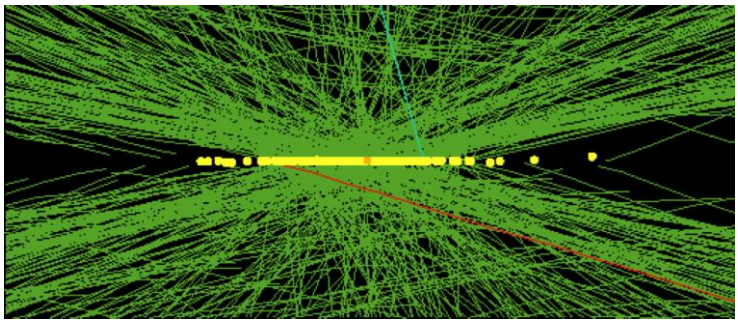

Figure 12: High pileup event with 78 reconstructed vertices taken in 2012 by CMS.

A relatively high-pileup crossing that was produced in a special data run in 2012 is shown in Fig. 12. There are 78 reconstructed vertices. The total number of pileup collisions is actually somewhat larger because some vertices have too few tracks to be reconstructed. The upgraded tracking systems can be designed with enough additional segmentation to associate charged particles with the correct interaction vertices most of the time, even for PU of 140 or 200. This enables the collision containing the hard scatter to be correctly reconstructed and for isolated leptons to be correctly identified in most cases.

3.3 Overview of the ATLAS upgrades

The harsher radiation environment and higher detector occupancies at the HL-LHC imply major changes to most of the ATLAS systems, especially those at low radii and large pseudorapidity. A general guideline for these changes is maintaining the same or improve the detector performance measured at the LHC. The higher event rates and event sizes will be a challenge for the trigger and data acquisition (DAQ) systems, which will require a significant extension of their capacity.
A Schematic view of the ATLAS detector with the various sub-systems is given in Figure 13. The ATLAS upgrade will be gradual and flexible to accommodate a possible evolution of LHC operational parameters and indications of new physics signals. It is planned in three phases, which correspond to the three long technical shutdowns of the LHC towards the HL-LHC.

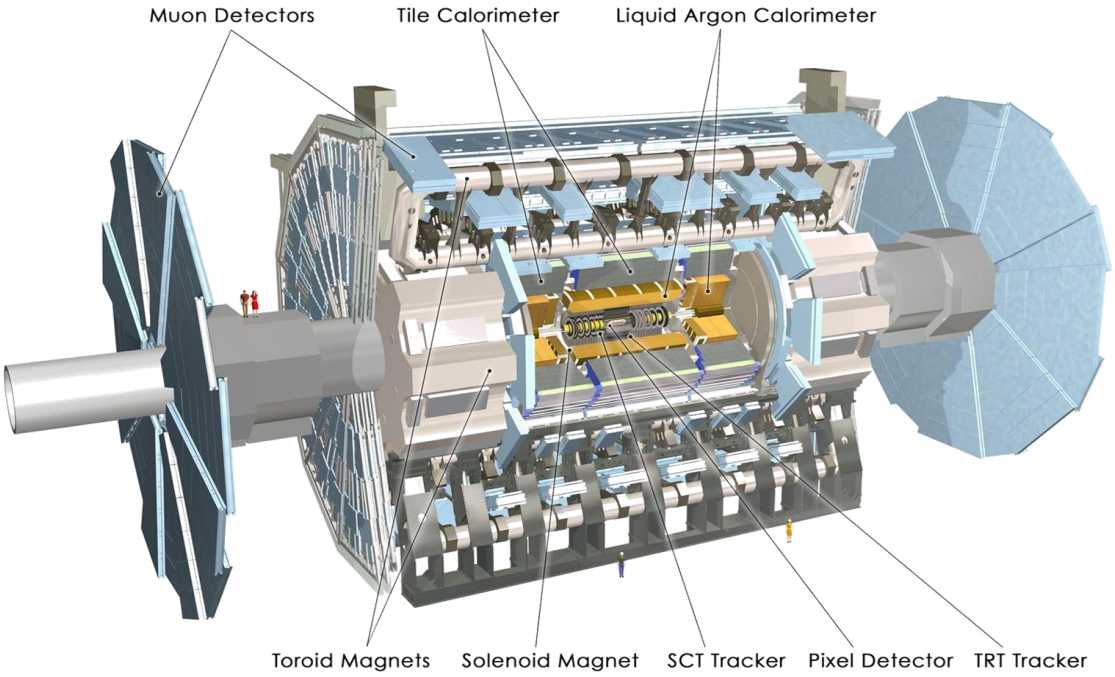

Figure 13: Schematic view of the ATLAS detector with the various sub-systems. The dimensions of the detector are 25m in height and 44m in length. The overall weight of the detector is about 7000 tons.

3.3.1 Phase-0 upgrades

ATLAS has used the shutdown period (Phase-0) for detector consolidation works, including a new Inner Detector (ID) cooling system, a new diamond beam monitor, the replacement of the Pixel internal services, new power supplies for the calorimeter, an improved coverage of the Muon Spectrometer (MS) between the barrel and the end-cap regions and a new beam pipe, in the central and forward region. But the main upgrade activity in Phase-0 is the installation of a new barrel layer in the Pixel detector. The Insertable B-Layer (IBL) is an additional, 4th pixel layer, that has been built around the new central beam pipe and then slipped inside the present Pixel detector in situ. The IBL is therefore placed between the actual innermost pixel layer (the B-layer) and the beam pipe, at a sensor average radius of 33 mm (50.5 mm is the radius of the B-layer). To make the installation of the IBL possible, the new Be beam pipe radius is reduced by 4 mm radius from 29 mm to 25 mm. IBL will help to preserve the tracking performance at high luminosity when the B-layer will suffer from radiation damage and high pile-up occupancies. Moreover, it will compensate for defects (irreparable failures of modules) in the existing detector, assuring tracking robustness. Given the closer position to the impact point and the smaller pixel size, IBL will also improve the vertex resolution, secondary vertex finding and b-tagging, hence extending the reach of the physics analysis.

3.3.2 Phase-I upgrades

A second shutdown (LS2) is being planned in 2019 to integrate the Linac4 into the injector complex, to increase the energy of the PS Booster to reduce the beam emittance, and to upgrade the collider collimation system. When data taking resumes in 2020, the peak luminosity is expected to reach about 2-3 x 10^{34}/cm^2/s corresponding to 55 to 80 interactions per crossing (pile-up) with 25 ns bunch spacing, well beyond the initial design goals. LHC is planning to deliver an integrated luminosity of about 300/fb before the next shutdown, thus extending the reach for discovery of new physics and the ability to study new phenomena and states. In this long shutdown, so-called Phase-I, ATLAS proposes the installation of new muon Small Wheels and several updates for the trigger system to handle luminosities well beyond the nominal values. Detailed plans are described in Ref. [7].

New Small Wheels: At high luminosity the performance of the muon tracking chambers (in particular in the end-cap region) degrades with the expected increase of cavern background rate. Moreover, in the current detector, the Level-1 muon trigger in the end-cap region is based on track segments in the intermediate muon station located after the end-cap toroid magnet. An analysis of 2012 data demonstrated that approximately 90% of the muon triggers in the end-caps are fake or background, dominated by low energy particles, mainly protons, generated in the material located between the Small Wheel and the middle station, hitting the end-cap trigger chambers at an angle similar to that of real high p_T muons. Therefore, to face with the large expected rates of the LHC upgrades, a replacement of the first endcap station of the Muon Spectrometer, the New Small Wheel (NSW), is proposed. The NSW must ensure efficient tracking at high particle rate of up to 5 x 10^{34}/cm^2/s and larger $|\eta|$, with position resolution of < 100 μm.
The NSW will have two chamber technologies, one primarily devoted to the Level-1 trigger function (small-strip Thin Gap Chambers, sTGC) and one dedicated to precision tracking (MicroMegas detectors, MM). The sTGC are primarily deployed for triggering given their single bunch crossing identification capability. The MM detectors have exceptional precision tracking capabilities due to their small gap (5 mm) and strip pitch (approximately 0.5 mm). Such a precision is crucial to maintain the current ATLAS muon momentum resolution in the high background environment of the upgraded LHC.

Level-1 LAr Calorimeter Electronics: Also the calorimetric trigger will have an upgrade in Phase-1: the objective of this upgrade is to provide higher-granularity, higher-resolution and longitudinal shower information from the calorimeter to the Level-1 trigger processors. The 10-fold increase in granularity will improve the trigger energy resolution and efficiency for selecting electrons, photons, τ-leptons, jets and missing p_T, while enhancing discrimination against backgrounds and fakes.

Fast Track Trigger (FTK): The Fast TracKer Trigger will perform the track finding and fitting online using dedicated massive parallel processing, which makes it extremely faster, instead of the Level-2 software farm as in the current trigger schema. FTK will then provide the track parameters with resolution close to the offline one shortly after the start of the Level-2 processing thus releasing extra resources for more advanced selection algorithms, which ultimately could improve the performances of the tracking-based filter algorithms such as the b-tagging and τ-trigger. While the full geometrical coverage for full Phase-I pile-up in foreseen after LS2, a progressive coverage and commissioning will start already in 2015.

Trigger and Data Acquisition: New calorimeter feature extraction processors and a new processor for the muon signals will produce object quantities that can be combined with each other and other signals in a new topological processor. The Data Acquisition and the High-Level Trigger (HLT) processing farm will be upgraded to allow full calorimetry information and the outputs of the FTK system to be read out and processed.

3.3.3 Phase-II upgrades

The Phase-I upgrades are designed to be fully forward-compatible with the physics program of the high luminosity HL-LHC (Phase-II), when the instantaneous luminosity should reach 5-7 x $10^{34}/cm^2/s$, up to 200 interactions per crossing (pile-up) and a total integrated luminosity of 3000/fb. A third 36-months long shutdown (LS3) in 2024-26 will be necessary to upgrade the accelerator to this ultimate operation mode. Detailed plans are described in Ref. [8].

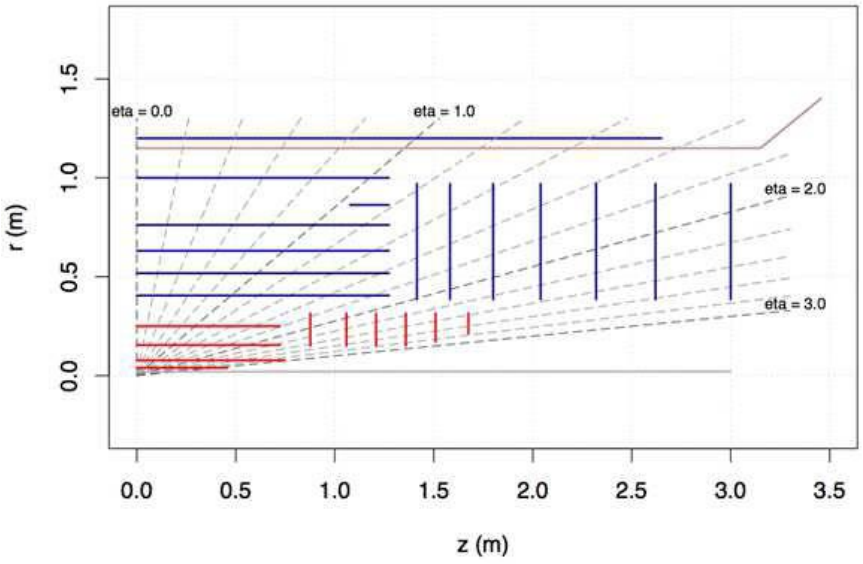

Figure 14: The proposed baseline layout design for the ATLAS inner tracker (ITK) in the Phase II upgrade. The ITK will be entirely a silicon detector. It consists of two main sections. Pixels in red and Strips in blue. The final silicon layer extends to 1m radius.

New Inner Tracker: The present ATLAS Inner tracker will have several limitations in Phase-II when up to 200 pile-up events per bunch crossing are expected. The gas-based TRT (Transition Radiation Tracker, the outermost system of the ATLAS Inner Detector) has a limit due to instantaneous luminosity because of very high occupancy. The functionality of the silicon-based parts of the tracker will be deteriorated due to the total radiation dose affecting both sensors and read-out electronics and also by the instantaneous luminosity, too high for the present limited band-width. Because of all these factors, the entire Inner Detector will be replaced with a new, all-silicon Inner Tracker (ITk) with pixel sensors at the inner radii surrounded by microstrip sensors. The current baseline design of the ITk, with a layout similar to the present detector, has in the central region sensors arranged in cylinders, with 4 pixel layers followed by 3 short-strip layers then 2 long-strip layers; the forward regions will be covered by 6 pixel disks and 7 strip disks. A schematic of the baseline layout for the ITK is shown in Figure 14. Notice the “stub layer” in the barrel region at 45 degrees with respect to the beam line and just inside the last barrel. This high services-to-sensor ratio layer is needed to maintain efficiency for tracking pattern recognition. The ATLAS inner tracker is a strip and pixel system, both consisting of a barrel and each has two end-caps to provide tracking coverage at high $|\eta|$. There are three main working groups associated with different sensor technologies and different detector geographical locations. These are pixels, barrel strips, and end-cap strips systems. A great deal of the design expertise in mechanical, electrical, and thermal management systems is shared between the working groups. The mechanical design in all systems assumes that the unit which will be constructed at remote institutions will follow a stave-concept. This is a long row of sensor modules with electrical and thermal management services integrated within the mechanical mounting structure. All of the services have connection points at the end of the stave. In all ITK subsystems cooling will be supplied by a recirculating CO_2 system that will achieve a sensor temperature of $\simeq -25^{\circ}C$. This long stave unit is designed to be inserted within the already-present barrel or wheel supports at CERN. This is a very different model than employed for the original ATLAS tracker where entire barrel cylinders were assembled and instrumented remotely and then shipped to CERN for final assembly.

The muon and electron trigger upgrades: A new trigger architecture is being developed that is compatible with the constraints imposed by the detector and provides a flexible trigger with the potential to deliver the required performance. As currently envisaged, the baseline design for the Phase-II Trigger, schematically sketched in Fig. 15, foresees a split Level-0/Level-1 hardware trigger with a total level-1 accept rate of 200 kHz and total latency of 20 μs. The Level-0 trigger would distribute the Level-0 accept at a rate of at least 500 kHz within a latency of 6 μs. The Phase-II Level-0 trigger is functionally the same as the Phase-I Level-1 system, based only on calorimetric and muon inputs. The Level-0 accept is generated by the central trigger system which incorporates topological triggering capability. The Level-1 system will reduce the rate to 200 kHz within an additional latency of 14 μs. This reduction will be accomplished by the introduction of track information within a Region-of-Interest (RoI), full calorimeter granularity within the same RoI and the introduction of a refined muon selection based on the use of the MDT information. All the trigger electronics of the calorimeters and muon spectrometer will need to be upgraded to face these trigger rates. Moreover the calorimeter electronics will also undergo changes to allow 40 MHz read-out of all the data without on-detector buffering.

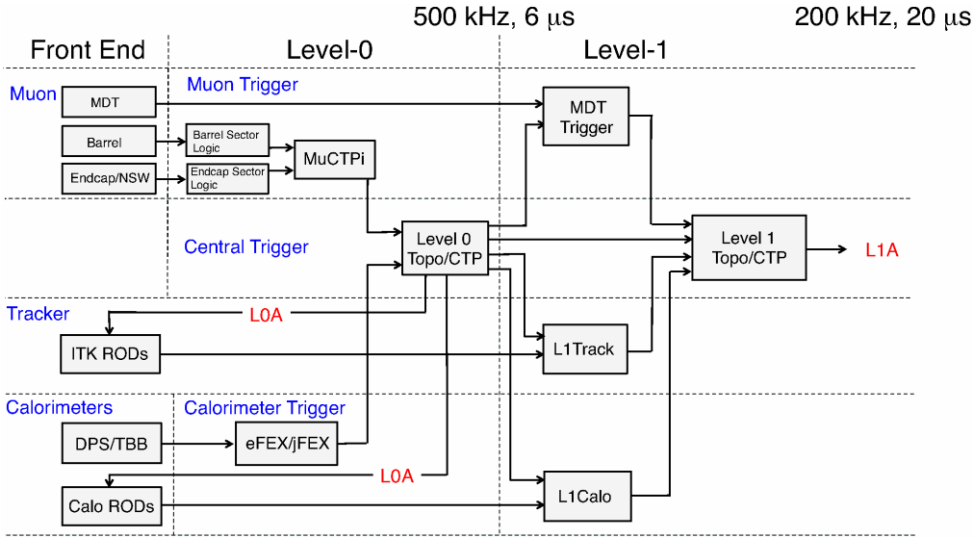

Figure 15: A block diagram of the architecture of the split Level-0/Level-1 hardware trigger proposed for the Phase-II upgrade.

3.4 Overview of the CMS upgrade

An exploded view of the CMS detector is shown in Fig. 16. At the heart of the experiment is a 13 m long, 6 m diameter, 4T superconducting solenoid providing large bending power for momentum measurements and whose return field is large enough to saturate the iron plates in the return yoke, enabling it to be used for muon momentum reconstruction. The bore of the magnet is large enough to accommodate the tracking and calorimetry systems. The tracking volume is contained in a cylinder of 5.8 m length and 2.6 m in diameter.

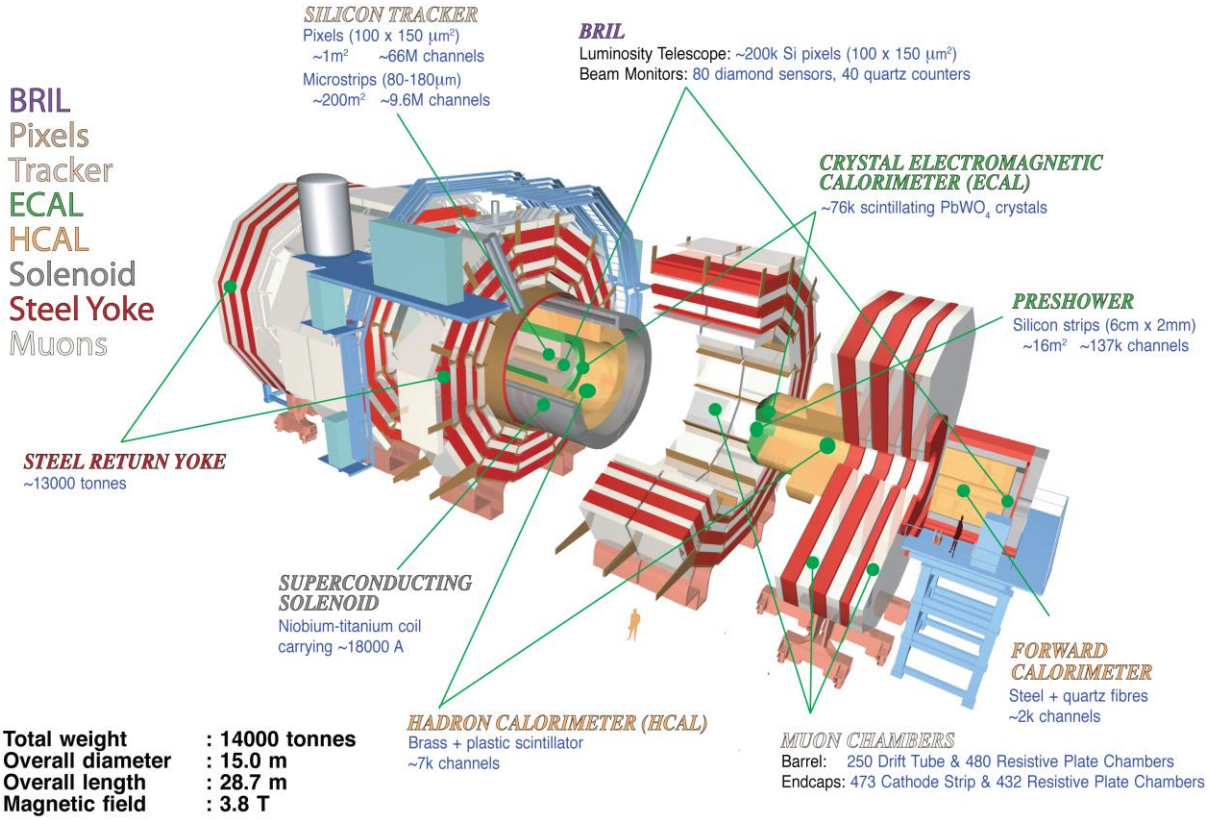

Figure 16: A schematic representation of the CMS Detector in with its various sections in retracted positions. The central yoke block is YB0. The first block (YB+1, and corresponding YB-1) is shown partially moved away from YB0. The second yoke block (YB+2, which has a corresponding YB-2) is shown fully moved past the solenoid vacuum tank. The endcap calorimeters are attached to the first endcap disk YE+1, then endcap CSCs and RPCs, then YE+2, more muon chambers, and YE+3, with additional muon chambers on the front and back. Eventually, another disk, YE+4 will be added at the end to provide shielding from beam related backgrounds. This configuration is repeated on the other end. In operation the detector is closed by moving all pieces together.

3.4.1 General considerations for the CMS phase-II upgrade

The primary goal of the upgrade program is therefore to maintain the excellent performance of the present detector under these challenging conditions throughout the extended operation of HL-LHC. A major focus of CMS has been to identify changes that are mandatory for the beam conditions of HL-LHC and significant effort has been expended to understand the effect of radiation damage. Performance projections are based on a combination of detailed measurements using the data taken in the experiment throughout the period 2011-2012 and the exposure of test components to radiation levels matching anticipated HL-LHC doses. From these studies it is very clear that the tracker and the endcap calorimeters must be replaced. Details of the CMS upgrade are discussed in Ref. [9].

With these required changes, the performance issues associated with high PU, that are also the most pronounced in the inner and forward detector regions, can be addressed. Pile-up mitigation in CMS heavily relies upon particle-flow event reconstruction. To this end, the tracker granularity can be increased to maintain the excellent tracking efficiency to enable the determination of the original *pp* collision points for all charged particles. New endcap calorimeter configurations will also provide the opportunity to optimize segmentation and improve energy resolution, particularly for jets. The ability to ensure efficient event selection for data acquisition is a key prerequisite to fully benefit from increased luminosity. The precise study of the relatively low-mass Higgs boson and the search for new particles occurring in cascade decays will require continued use of low transverse momentum, p_T, trigger thresholds. To achieve this, the trigger electronics (i.e. the L1 trigger) must be upgraded. A

sufficient reduction in trigger rate can only be accomplished by improving p_T resolution to obtain lower rates without loss of efficiency, and by mitigating the effect of the combinatorial backgrounds arising from PU. A new approach is therefore required, namely the introduction of tracking information at L1, providing the capability to implement trigger algorithms similar to that of the current HLT, including the use of precise momentum measurements. Facilitating tracking in the L1 trigger is an important driver of the design of the Phase-II Tracker. The upgraded L1 "track trigger" will require a new hardware architecture to incorporate the tracking information. While the addition of track information in the L1 trigger provides significant gains in rate reduction with good efficiency, it will nevertheless be necessary to increase the trigger accept rate in order to maintain the required efficiency for all of the important physics channels. This is particularly the case for triggers involving hadrons and photons, for which the sensitivity to PU is higher and the track trigger is somewhat less efficient.

The measurement of processes with small production cross-sections and/or decay branching ratios is a major goal of the HL-LHC physics program. This requires specific upgrades in the forward regions of the detector to maximize the physics acceptance over the largest solid angle possible. To ensure proper trigger performance within the present coverage, the muon system will be completed with new chambers. The new endcap calorimeter configuration offers the opportunity to extend the muon coverage with a tagging station up to $|\eta| \approx 3$ or more, with significant acceptance gain for multi-muon final states. To mitigate PU effects in jet identification and energy measurement, the tracker will be extended up to $|\eta| \approx 4$, thereby also covering the peak production region of jets accompanying Vector Boson Fusion (VBF) and Vector Boson Scattering (VBS) processes, which are among the highest priorities of the physics program. With this extension, measurements of total energy and missing energy will be greatly improved, and b-tagging acceptance will be increased.

As the luminosity integrated over the Phase-II operation period will not be limited by the accelerator performance but by the ability of the detector to sustain high PU, the upgrades of the readout electronics will be designed with some margin to allow efficient data taking up to a PU of 200. This will also provide some flexibility for the luminosity levelling process to use instantaneous luminosity and corresponding beam lifetime information to maximize the useful integrated luminosity in order to obtain the best possible physics performance of the experiment. It is expected that the sustainable luminosity limit will be driven by the performance of sub-detectors that are not going to be replaced for Phase-II. Further simulation studies will include possible alternatives to the luminosity levelling schemes and PU beyond 140 to further optimize designs and to determine the best operating scenarios. Among the studies foreseen, CMS will investigate whether or not precise measurements of the production time of particles, which vary with a rms of ~200 ps within a single bunch crossing, would enable a valuable improvement in PU mitigation, particularly for the contributions of neutral particles, which are not detected in the tracker.

3.4.2 Elements of the CMS phase-II upgrade

Tracker: The Tracker will suffer significant radiation damage by LS3 and must be completely replaced for Phase-II. To maintain adequate track reconstruction performance at the much higher PU levels of the HL-LHC, the granularity of both the outer tracker and the pixel systems will be increased by roughly a factor 4. In the outer tracker, this will be achieved by shortening the lengths of silicon sensor strips relative to those in the current detector, without changing the pitch very significantly. A number of design improvements will lead to a much lighter Outer Tracker providing significantly improved p_T resolution and a lower rate of γ-conversions compared to the present detector. In addition, the module design will be capable of providing track-stub information to the L1 trigger at 40 MHz for tracks with $p_T \geq 2$ GeV/c. This will ensure powerful background rejection at the earliest stage of the event selection. The pixel system will implement smaller pixels and thinner sensors for improved impact parameter resolution and better two-track separation. This will improve *b*-tagging as well as τ-

hadronic decay and track reconstruction efficiencies within boosted jets. With up to 10 additional pixel disks in each of the forward regions the system coverage will be extended to close to $|\eta| \approx 4$, to better match the range of coverage of the calorimetry. A sketch of one quadrant together with the planned granularity is shown in Fig. 17.

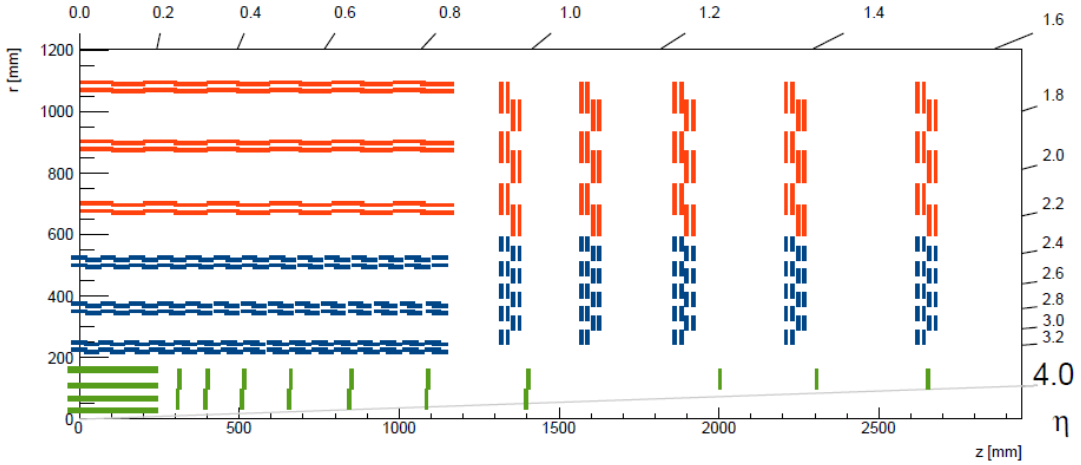

Figure 17: Sketch of one quarter of the Tracker layout. Outer Tracker: red lines correspond to strip modules with 90 µm pitch and 5 cm length; blue lines to macro-pixels with 100 µm pitch and 2.5 cm length or 100 µm and 1.5 mm length, depending on the radial distance from the bema-line. The Inner Pixel detector, with forward extension, is shown in green and has a pixel sizes of 25 x 100 µm^2 or 50 x 50 µm^2.

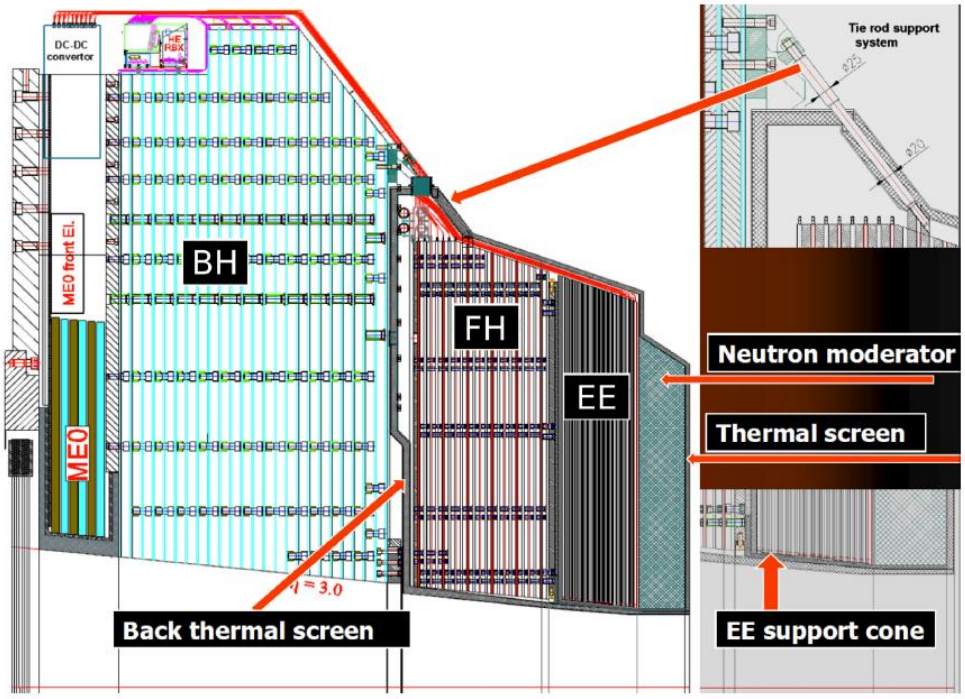

Figure 18: Technical drawing of the overall endcap calorimeter structure. The electromagnetic part of the endcap calorimeter (EE) has its front face at the same location as the front face of the current EE. Directly behind it is the silicon-brass calorimeter (FH). Behind that is a 5λ backing hadron calorimeter (BH), which, since the radiation levels are low, uses a similar technology to that of the current hadron endcap calorimeter HE.

Calorimeter endcaps: The electromagnetic and hadronic endcap calorimeters will also suffer significant radiation damage by LS3, and so must be replaced. The replacement is called the High Granularity Calorimeter (HGC) and has electromagnetic and hadronic sections with excellent transverse and longitudinal segmentation. It will provide detailed three dimensional images of showers. The electromagnetic section consists of ~30 tungsten and copper plates interleaved with

silicon sensors as the active material. The sensors have pads of variable sizes of less than ~1.0cm^2. The electromagnetic section has 25 X_0 and one interaction length (λ). The hadronic part has a front section of 12 brass and copper plates interleaved with silicon sensors for a depth of 3.5λ. This covers the hadronic shower maximum measurement. It is followed by a "backing hadron calorimeter" of similar design to the current HE detector, brass plates interleaved with plastic scintillating tiles read out with a wavelength shifting fiber, to provide an overall depth of 10λ for the full calorimeter. The design of the High Granularity Calorimeter draws upon the ILC/CALICE concepts for 3D measurement of shower topologies and is shown in Fig. 18.

Muon endcaps: The muon system in the region $1.5 \leq |\eta| \leq 2.4$ currently consists of four stations of Cathode Strip Chambers (CSC). It is the only region of the muon detector that lacks redundant coverage despite the fact that it is a challenging region for muons in terms of backgrounds and momentum resolution. To maintain good L1 muon trigger acceptance in this region it is therefore proposed to enhance these four stations with additional chambers that make use of new detector technologies with higher rate capability, along the lines of what was planned in the original design of CMS. The two first stations are in a region where the magnetic field is still reasonably high and so will use Gas Electron Multiplier (GEM) chambers for good position resolution in order to improve momentum resolution for the standalone muon trigger and to improve the matching with tracks in the global muon trigger. The two last stations will use low-resistivity Resistive Plate Chambers (RPC) with lower granularity but good timing resolution to mitigate background effects. In addition, the implementation of a GEM station in the space that becomes free behind the new endcap calorimeters is being proposed in order to increase the coverage for muon detection to $|\eta| \approx 3$.

Beam radiation protection and luminosity measurement: The systems that provide protection against beam background and measurement of the luminosity will require work in several areas to manage the high radiation levels of the HL-LHC. The protection systems will be upgraded with new poly-crystalline diamond sensors that will be read out using the standard LHC Beam Loss Monitor hardware and software and fully integrated into the LHC control system. The Machine Induced Background (MIB) and Luminosity measuring systems in the Pixel volume must also be replaced.

Trigger: The latency of the present L1 trigger is limited to 3.4μs by the tracker readout. For Phase-II operation, it will be increased to 12.5μs to provide sufficient time for the hardware track re-construction and matching of tracks to muons and calorimeter information. This change will require upgrades of the readout electronics in some of the existing sub-detectors that will be kept for Phase-II. A proper design of the front-end electronics for these systems will allow latency limitations to be overcome and at the same time to eliminate L1-trigger rate restrictions. Based on the expected performance of the trigger with track information, the proposed L1- trigger acceptance rate is 500 kHz for beam conditions yielding 140 PU. This will allow CMS to maintain thresholds comparable to those that will be used in a typical Phase-I trigger menu. To retain comparable performance in beam conditions that result in 200 PU, the L1 rate must increase to 750 kHz, and so all detectors will have readout capabilities compatible with this possibility. Studies are underway to optimize scenarios for the trigger menu and to determine if a higher acceptance rate would further improve the exploitation of the higher luminosity for key physics signals. Any further increase of the L1 readout rate would require an increase of the Pixel readout bandwidth. Specific sub-detector upgrades also required for CMS to meet these trigger requirements are the front-end electronics of the barrel calorimeter; the Muon readout electronics in the CSCs of the inner rings in stations 2 to 4; and the DT readout.

Data Acquisition and Trigger Control: The Data Acquisition (DAQ) system will be upgraded to implement the increase of bandwidth and computing power that will be required to accommodate the larger event size and L1-trigger rate, and the greater complexity of the reconstruction at high PU. Compared to Phase-I, the bandwidth and the computing power requirements would respectively

increase by factors of about 10(15) and 15(30) for operation at PU of 140(200). This is well within the projected network and computing technology capabilities expected at the time of Phase-II. Assuming an online event selection of 1/100 event at the HLT, as is the case in the current system, the subsequent rate of recorded data will increase at PU of 140(200) to 5(7.5) kHz from LHC Run-I levels of roughly a few hundred Hz.

Software and Computing: Assuming only technology improvements and maintaining existing techniques, the offline software and computing areas would fall short by a factor of 4(12) of the resources needed for the challenging conditions expected in Phase-II at 140(200) pileup.
To minimize the computing needs, both at the online and offline levels, a significant R&D program has started as part of the upgrade effort to improve the algorithms and approaches used for data reconstruction, analysis, storage, and access and to adapt the CMS software and computing model to new technologies and resources.

4. Flavour physics and the upgrade of LHCb

The large production cross-sections for heavy flavoured particles in LHC *pp* collisions provide excellent opportunities for heavy flavour physics. In particular, precision measurements of rare decays and *CP* violation allow studies of effects of virtual particles that can contribute to quantum loops. Certain observables can be predicted with low uncertainty in the standard model, and provide sensitivity to new physics even if it occurs at energy scales far above those that can be directly probed by the LHC. Since the effects of new physics in flavour observables depend on the complex coupling coefficients as well as the energy scale, these measurements are complementary to the energy frontier searches, and thus increase the discovery potential of the LHC.
The use of the LHC to make precision measurement in the heavy flavour sector has been definitively proved by the results from Run I data. The dedicated heavy flavour experiment LHCb has produced a range of world-leading results for *B* and *D* meson oscillations, *CP* violation and rare decays. The results from ATLAS and CMS in the beauty sector are limited mainly to final states containing dimuons, due to their stringent trigger constraints, but in those areas very significant contributions have been made. In addition, the large samples of top quarks available at ATLAS and CMS have brought studies of the heaviest flavour into the precision domain.
In order to exploit fully the flavour physics potential of the LHC, an upgrade to the LHCb detector has been proposed [10, 11] and approved. The upgraded detector will be installed in LS2 and commence operation in 2021. LHCb will then record data at an instantaneous luminosity of $2 \times 10^{33}/\text{cm}^2/\text{s}$, levelled using a scheme similar to that deployed during Run I. The LHCb upgrade design is qualified for an integrated luminosity of 50/fb, but it is anticipated that LHCb will continue to be operational throughout the HL-LHC era. The upgrades of ATLAS and CMS will also significantly enhance their heavy flavour physics capabilities, in particular the improvements to the tracking and muon detectors and the triggers. The Belle II experiment at the SuperKEKB e^+e^- collider in Japan will also accumulate large samples of beauty and charm hadrons, and pursue an extensive programme of flavour physics measurements with complementary sensitivity to the LHC experiments. Although a very wide range of interesting observables of the *b* and *c* hadrons, the τ lepton and the top quark can be studied with the HL-LHC, a small subset has been chosen to provide an illustrative range of sensitivity studies. These are each briefly described below.

4.1. Rare decays

Rare decays include exotic decays with lepton flavour or number violating decays and flavour changing neutral currents (FCNC) processes that are mediated by electroweak box and penguin diagrams in the SM. Among the interesting decays the $B^0_{s/d} \rightarrow \mu^+\mu^-$ is one of the most sensitive to NP since its branching ratio can be enhanced or reduced by new particles entering in the decay diagrams that compete with the standard model ones.

4.1.1. Ratio of branching fractions of $B^0 \to \mu^+\mu^-$ over $B_s^0 \to \mu^+\mu^-$ decays

In the HL-LHC era, one of the most interesting observables will be the relative branching fractions of the B^0 and B_s^0 di-muon decays. This will be measured by CMS and LHCb, and also by ATLAS if the improvement in mass resolution necessary to separate the B^0 and B_s^0 peaks can be achieved. With the upgraded LHCb detector the expected uncertainty on the $B_s^0 \to \mu^+\mu^-$ reaches 5% precision, but more importantly the error on the ratio of branching ratio, BR($B^0 \to \mu^+\mu^-$)/BR($B_s^0 \to \mu^+\mu^-$) will be of the order of 40% allowing to exclude several new physics models if no deviation is found. When large $B_s^0 \to \mu^+\mu^-$ samples are available, it will also be possible to go beyond branching fraction measurements and use additional handles on possible new physics contributions, such as the effective lifetime.

The sensitivities quoted in Table 2 are extrapolated from current results, assuming the SM value of the ratio of branching fractions. The extrapolation also takes into account some expected loss of efficiency due to the high pile-up conditions, and assumes that the trigger thresholds and analysis procedures will remain the same as those used for existing data. Systematic uncertainties which arise, for example, from the lack of knowledge of background decay modes containing misidentified hadrons, are expected to be controlled to better than the level of statistical precision.

4.1.2. Angular observables in the decay $B^0 \to K^{*0}\mu^+\mu^-$

The $B^0 \to K^{*0}\mu^+\mu^-$ decays provide a wide range of angular observables, many of which are predicted with low theoretical uncertainty in the SM. These observables probe the helicity structure of the SM and can be used not only to search for new physics effects, but to understand which operators are affected by the new physics. The latest results from LHCb show an interesting tension with the SM predictions. ATLAS and CMS have both also reported studies of $B^0 \to K^{*0}\mu^+\mu^-$ decays. One of the many interesting observables that can be studied in these decays is the point where the forward-backward asymmetry, A_{FB}, as a function of the di-muon invariant mass-squared, q^2, crosses zero. This will be determined by ATLAS, CMS and LHCb in the HL-LHC era. Sensitivity studies from ATLAS and CMS are, however, not available.

The expected sensitivities presented in Table 2 are based on extrapolating the yields of the current measurements while assuming the SM distribution of A_{FB} as a function of q^2.

4.2. *CP* violation

Understanding the violation of Charge conjugation and Parity (CP) is one of the key question in physics. In the SM *CP* violation enters via the CKM mechanism, which describes the current experimental data but it is known to generate insufficient *CP* violation to explain the baryon asymmetry in the Universe. The major part of models that extend the SM predict new sources of *CP* violation in particular in the *b* hadron system. The LHCb experiment has already studied several processes but in order to be sensitive to new physics effects a better precision is needed. One of the major goals of the experiment is the determination of γ, one of the angles of the unitarity triangle that is to date the least known.

4.2.1. CKM angle γ from $B \to DK$ decays

The angle γ of the CKM unitarity triangle, when determined from decays such as $B \to DK$ that contain only tree amplitudes, provides a SM benchmark measurement of *CP* violation with negligible theoretical uncertainty. Its precision determination is therefore one of the main goals of current and future flavour physics experiments including LHCb and Belle II. The latest results from LHCb give uncertainties of ±9.5°, while Belle obtain ±15°. Improvements in the determination of will be a major goal for LHCb. This includes not only improving the precision of the observables that are currently used in the combinations, but also adding additional channels that may make significant contributions when sufficiently large data samples are available. The expected sensitivities for LHCb and Belle II presented in Table 2 are based on extrapolating from current measurements. It is expected that it will be possible to control systematic uncertainties at better than the 1° level in both experiments.

Table 2: Expected sensitivities that can be achieved on key heavy flavour physics observables, using the total integrated luminosity recorded until the end of each LHC run period. Discussion of systematic uncertainties is given in the text. Uncertainties on φ_s are given in radians. The values for flavour-changing neutral-current top decays are expected 95% confidence level upper limits in the absence of signal.

		LHC era			HL-LHC era	
		Run 1	Run 2	Run 3	Run 4	Run 5+
$\frac{\mathcal{B}(B^0\to\mu^+\mu^-)}{\mathcal{B}(B_s^0\to\mu^+\mu^-)}$	CMS	$> 100\%$	71%	47%	...	21%
	LHCb	220%	110%	60%	40%	28%
$q_0^2\ A_{\rm FB}(K^{*0}\mu^+\mu^-)$	LHCb	10%	5%	2.8%	1.9%	1.3%
	Belle II	—	50%	7%	5%	—
$\phi_s(B_s^0\to J/\psi\phi)$	ATLAS	0.11	0.05–0.07	0.04–0.05	...	0.020
	LHCb	0.05	0.025	0.013	0.009	0.006
$\phi_s(B_s^0\to\phi\phi)$	LHCb	0.18	0.12	0.04	0.026	0.017
γ	LHCb	7°	4°	1.7°	1.1°	0.7°
	Belle II	—	11°	2°	1.5°	—
$A_\Gamma(D^0\to K^+K^-)$	LHCb	3.4×10^{-4}	2.2×10^{-4}	0.9×10^{-4}	0.5×10^{-4}	0.3×10^{-4}
	Belle II	—	18×10^{-4}	4–6×10^{-4}	3–5×10^{-4}	—
$t\to qZ$	ATLAS	...	...	23×10^{-5}	...	4.1–7.2×10^{-5}
	CMS	100×10^{-5}	...	27×10^{-5}	...	10×10^{-5}
$t\to q\gamma$	ATLAS	...	...	7.8×10^{-5}	...	1.3–2.5×10^{-5}

4.2.2. *CP* violation in B_s^0 oscillations

The *CP* violating phase in B_s^0 oscillations φ_s is very small in the SM (φ_s^{SM} = -0.0364±0.0016 rad) but can be enhanced in new physics models. The benchmark channel for the measurement is $B_s^0 \to J/\psi\ \varphi$. Significant improvement in the precision is warranted not only in this channel, but also in the loop-dominated $B_s^0 \to \varphi\varphi$ decay. A first measurement with this channel has been performed by LHCb. The experiments expect to continue studies of $B_s^0 \to J/\psi\ \varphi$ in the HL-LHC era.

ATLAS has performed a detailed analysis, extrapolating from existing data and taking into account the increased cross-sections for signal and background at $\sqrt{s}$ = 14 TeV, improvements in the decay time resolution arising from upgrades of the inner tracker, and the impact of the increased pile-up on resolution parameters. The effective tagging efficiency is assumed to remain the same as in existing data, and the measurement is assumed to remain statistically limited as the main systematic uncertainties is expected to scale with increased data samples. Another key parameter which affects the sensitivity is the p_T threshold used in the trigger for the online event selection.

The sensitivity projections for $B_s^0 \to J/\psi\ \varphi$ at LHCb assume similar performance to the current detector, with a modest improvement in the effective tagging efficiency. The systematic uncertainty in the current analysis is at the level of 0:01 rad, and is expected to be reduced further as larger data samples are accumulated. The projections for the hadronically-triggered $B_s^0 \to \varphi\varphi$ mode include also a factor due to the improved trigger efficiency expected with the high-level trigger of the LHCb upgrade. Similar sensitivity will also be achieved for the $B_s^0 \to K^{*0}\ K^{*0}$ mode, which probes similar physics. Table 2 summarizes the perspectives on the measurement of the angle φ_s at the HL-LHC.

4.3. The LHCb upgrade

The LHCb detector, shown in Fig. 19, is a single-arm spectrometer covering the pseudo-rapidity range of $2 < \eta < 5$. The experiment is fully instrumented in the whole acceptance, having excellent vertex- and mass-resolutions combined with particle identification over a large momentum range. LHCb profits from the very large heavy flavour production cross sections at LHC. Moreover, the majority of the *b* and *c* flavoured hadrons are produced in the very forward region. Even though LHCb only covers 4% of the solid angle, 40% of the $b\bar{b}$ pairs are produced within its acceptance.

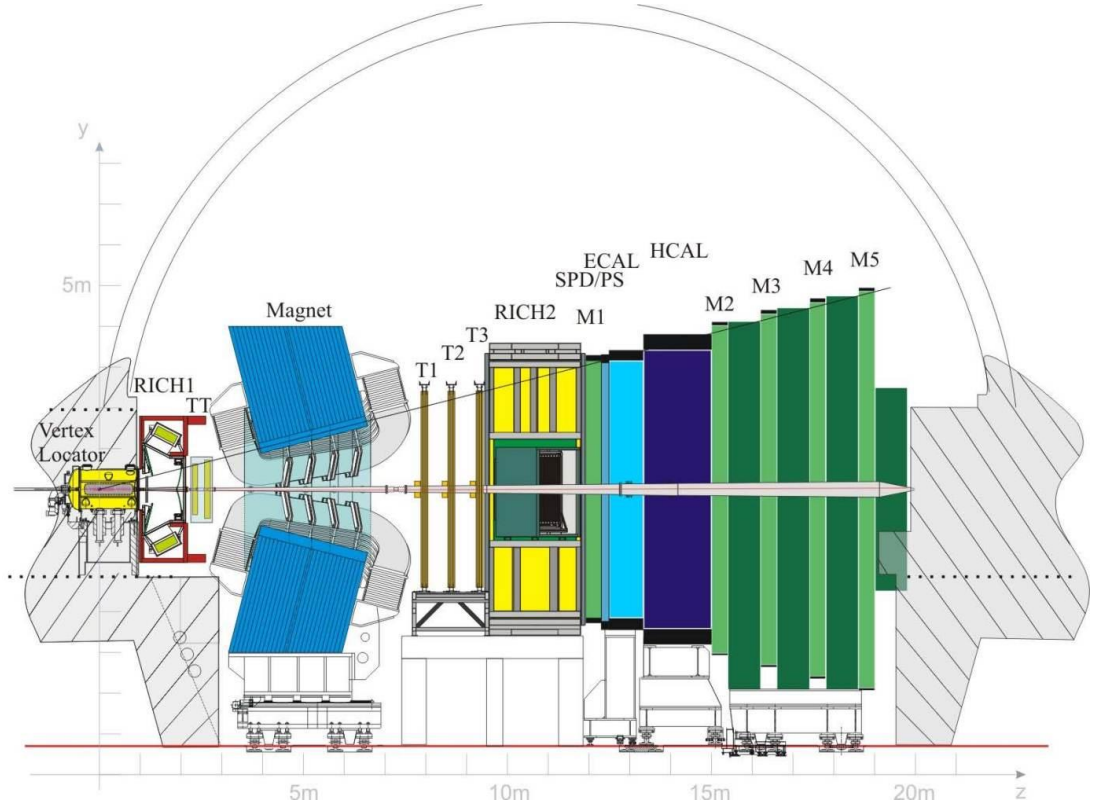

Figure 19: Schematic view of the LHCb upgrade detector. RICH1,2 = Ring Imaging Cherenkov detectors 1 and 2. TT= Tracker Turicensis. T1, T2, T3 = Tracking stations 1, 2 and 3. SPD/PS = Scintillating Pad Detector/Preshower. ECAL = Electromagnetic Calorimeter. HCAL = Hadron Calorimeter. M1, M2, M3, M4, M5 = Muon stations 1 to 5.

LHCb has access to a sample of heavy flavour decays of unprecedented size. This comes at the price of a more challenging experimental environment. Hence the event selection is crucial for the performance of the experiment, in particular the online selection performed by the trigger system. LHCb has shown that it performs very well in these challenging experimental conditions and that high precision measurements are possible at a hadron collider. The experiment took data at a luminosity of 4 x 10^{32}/cm^2/s during Run I, which is twice the design value but still significantly below what LHC could provide. A scheme of luminosity levelling has been devised where the beams are slightly displaced from head-on collisions and gradually re-centred during the fill as the beam intensity is reduced. This allows the experiment to collect data at a constant luminosity throughout the fill. LHCb is not limited by the luminosity that the LHC can deliver, but rather by the luminosity that could be turned in to high precision measurements. The aim of the LHCb Upgrade is to operate the experiment at a luminosity of 2 x 10^{33}/cm^2/s while increasing the efficiency of selecting signal candidates. The key features of the upgraded experiment, with which about 50/fb will be collected, is outlined in the following.

4.3.1. The LHCb trigger upgrade

The current limitations to perform measurements with higher precision are the Data Acquisition and the trigger. At present LHCb relies on a hardware based L0 trigger, which uses transverse energy and momentum criteria on electrons, photons, hadrons and muons to reduce the readout rate to 1MHz. The trigger thresholds are about 1 GeV/c for muons and 3-4 GeV/c for electrons, photons and hadrons. The High Level Trigger (HLT) then accesses the full detector information at 1 MHz and performs mainly inclusive selections by triggering on partially reconstructed decays. Physics processes are finally selected by fully reconstructed decays together with mass requirements. The High Level Trigger tasks run almost 30.000 independent copies of the executable on about 1600 CPU nodes. With an output

physics rate of 5kHz at $\sqrt{s}$ = 8TeV in run 1 this trigger configuration led to an efficiency of about 90% for *B* decays to muons, about 30% for *B* decays to hadrons and about 10% for charm decays.

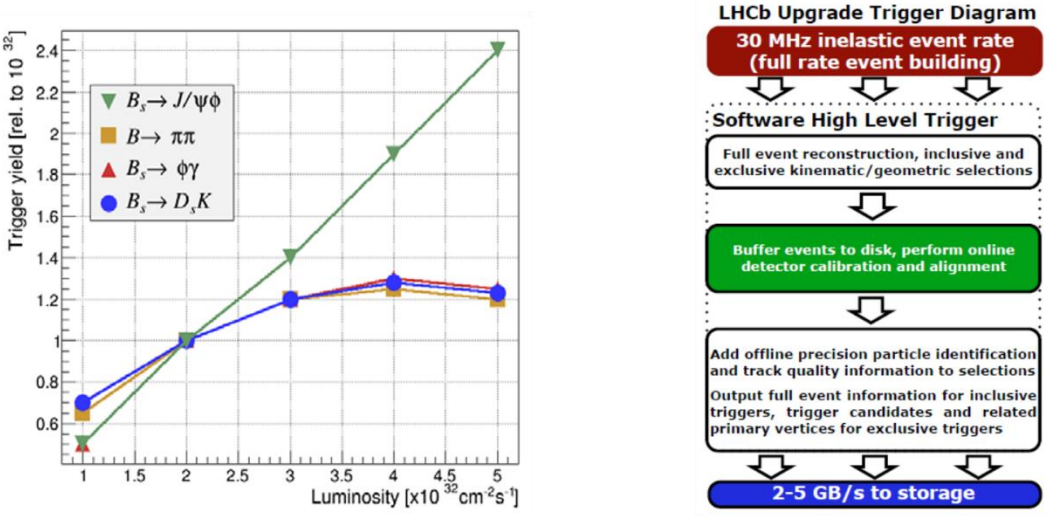

Figure 20: Left: Trigger yield for different *B* decays as function of the instantaneous luminosity. Only *B* decays triggered by with muons in the final state do not saturate. Right: Schematic view of the full software trigger.

At a centre of mass energy of 14 TeV and a luminosity of 2 x 10^{33}/cm^2/s the fake rate will increase drastically and in order to stay within the reserved trigger bandwidth, the cuts on the transverse energy must be increased, with the inevitable consequence of reducing the signal yield. Figure 16 shows the trigger yields as function of the instantaneous luminosity for different decay channels. While modes with muons are sufficiently clean to be handled efficiently even at high luminosity values, the hadronic modes reach already at low luminosity a saturation level due to the combinatorial effects and the Level 0 trigger bandwidth limitation. Hence, an efficient trigger selection requires necessarily a reconstruction with information from the entire detector and removing the Level 0. The LHCb upgrade strategy therefore consists of reading out the entire detector at 40MHz, with a fully software trigger keeping the luminosity levelled at 1-2 x 10^{33}/cm^2/s. The consequence of the 40 MHz readout is that all the sub-detector Front-End and Back-End electronics must be replaced and the detectors with embedded electronics have to be rebuilt. Furthermore the detector components have to be adapted to the increased occupancies. The aim is to reduce the 40 MHz collision rate in the Event Filter Farm to an event rate of 20-100 kHz to be written to tape, as shown in Fig. 20. The yield of muonic final states will increase by a factor 10, and the one of hadronic channels by a factor 20 compared to the current experiment. Details are given in the Online and Trigger Technical Design Report (TDR) [12].

4.3.2. Detector upgrade

The major changes will involve replacement of the tracking system and significant modifications of the particle identification detectors. The VErtex Locator (VELO), the Trigger Tracker (TT) detector and the T-stations (T1/2/3) will be completely replaced with the goal of to keeping the current performances for track reconstruction and vertex finding, but in harsher conditions.

VELO Upgrade: The new VELO, as the previous one, is essential for offline track and vertices identification and it is very important to reconstruct efficiently and quickly tracks at the trigger level to reduce the large minimum bias rate. Planar silicon pixel of 55x55 $\mu m2$ will be used, increasing the granularity and consequently the spatial resolution. Since the impact parameter resolution is dominated by the radius of the first measured point and the material distribution, to determine the best configuration a simulation has been performed including all the passive and active detector elements. From these studies it has been determined that the sensor distance to the beam will be

reduced by 2*mm* such that the inner radius will be about 3.5mm from the beam instead of 5.5*mm*. This will allow not only to improve the impact parameter resolution and but also to increase the track acceptance. The new pixel detector will be readout at 40 MHz by a new radiation hard ASIC chip capable to handle the large radiation dose, up to 5 x 10^{15} 1 MeV neutron equivalent fluence, and to cope with the expected data rates. Further challenges are to implement the on-chip zero-suppression in the front-end ASIC. The upgraded VELO will reuse large parts of the current mechanical infrastructure, in particular the vacuum tank and part of the cooling system which will be an innovative evaporative microchannel CO_2 cooling. Details are discussed in the LHCb VELO TDR [13].

Tracker Upgrade: The current Trigger Tracker will be replaced using silicon micro-strips with higher segmentation in order to reduce the occupancy and ghost tracks rate. The acceptance will be improved moving the sensors closer to the beam pipe and adapting their shape. The sensors thickness will go from 500µm to 300µm to reduce the material budget. This new Upstream Tracker (UT) should allow a fast VELO-UT track identification and it should efficiently resolve fake tracks reconstructed between the VELO and the main tracking stations after the magnet.
The upgrade of the tracking stations downstream the magnet aims mainly at reducing the occupancy in the inner region in order to maintain the same offline tracking performances as of Run I, and to provide a fast tracking algorithm for the trigger. The LHCb collaboration scintillating fiber tracker. The detector area of 5m by 6m will be covered by layers of scintillating fibres with a diameter of 250 µm and read out via Silicon Photo-Multipliers (SiPMs). The expected spatial resolution is about 60-100 µm. The design and expected performance are summarized in the Tracker Upgrade TDR [14].

Particle Identification System: The particle identification system (PID) is constituted by two RICH detectors, the muon chambers and the calorimeter detectors. In the case of the two RICH systems the hybrid photomultipliers (HPD) will be replaced by multi-anode photomultipliers since the FE electronics is integrated in the HPDs. The first muon detector layer together with the scintillating pad and pre-shower detectors used to separate electrons from photons with the calorimeter, will be removed due to their very high occupancy. These detectors were essential for the Level 0 trigger that now is removed. In order to run at high luminosity, the calorimeters will only reduce the gain on the photomultipliers and compensate with an increased electronics gain. These facts together with the full electron and gamma reconstruction in the HLT are expected to improve the resolution of the electromagnetic calorimeter helping in *e/γ* separation. The muon detectors after the calorimeters will remain as they are. Design and expected performance are summarized in the LHCb PID TDR [15].

The target is to install and commission the upgraded detector in the second long LHC shut down, scheduled for 2019-2020.

5. Heavy-Ion Physics and the ALICE upgrade

While ground-breaking measurements on the properties of strongly interacting matter in *pp, p*Pb and PbPb collisions at the LHC are being performed, it is clear that many important questions in heavy-ion physics will remain unanswered in this first phase of beam times up to 2018. ALICE is setting up a program of detector upgrades to be installed in the LHC shutdown 2 planned for 2019-2020, to address the new scientific challenges, and also the other experiments plan major upgrades, as mentioned in previous sections. The goal of the experiments is to integrate, for PbPb collisions at $\sqrt{s_{NN}}$= 5.5 TeV, an integrated luminosity Lint exceeding 10/nb after LS2. This represents an increase by an order of magnitude with respect to the expectation for Run 2 (between LS1 and LS2). In the case of the ALICE experiment, the upgrade of the detector read-out capabilities will allow for the recording of all interactions with a minimum bias trigger, up to a rate of 50 kHz. This will allow for an increase in the data sample by two orders of magnitude, which is crucial for the main points of the ALICE upgrade programme, as illustrated below.

In the second generation of LHC heavy-ion studies following LS2, the investigation of strongly interacting matter at high temperature and energy density will focus on rare probes, and on the study of their coupling with the medium and of their hadronization processes. These include heavy-flavour particles, quarkonium states, jets and their correlations with other probes, as well as real and virtual photons. The collaborations are developing second-generation heavy-ion physics programmes with a high level of complementarity, which will allow us to exploit at best the increased LHC luminosity for ion beams.
The main items of these programmes are listed in the following. Most of them will be addressed by all experiments, with focus on different kinematic regions.

5.1. Main topics in heavy ion physics at the HL-LHC

Heavy flavour: precise characterization of the quark mass dependence of in-medium parton energy loss; study of the transport and possible thermalization of heavy quarks in the medium; study of heavy quark hadronization mechanisms in a partonic environment. These require measurements of the production and azimuthal anisotropy of several charm and beauty hadron species, over a broad momentum range, as well as of *b*-tagged jets. ALICE and LHCb will focus on the low-momentum region, down to even zero p_T in the case of ALICE, and on reconstruction of several heavy flavour hadron species. ATLAS and CMS will focus mainly on *b*-tagged jets, and LHCb on J/ψ from *B*-decays. Initial-state effects in pPb collisions will also be investigated through heavy flavour.

Quarkonia: study of quarkonium dissociation and possible regeneration as probes of deconfinement and of the medium temperature. ALICE will carry out precise measurements, starting from zero p_T, of J/ψ yields and azimuthal anisotropy, ψ' and Υ yields, at both central and forward rapidity. ATLAS and CMS will carry out precise multi-differential measurements of the Υ, Υ', Υ'' states to map the dependencies of their suppression pattern. They will also extend charmonium measurements to high transverse momentum. Initial-state effects through precise measurement of quarkonia in pPb collisions will also be investigated.

Jets: detailed characterization of the in-medium parton energy loss mechanism that provides both a testing ground for the multi-particle aspects of QCD and a probe of the QGP density. The relevant observables are: jet structure and di-jet imbalance at TeV energies, b-tagged jets and jet correlations with photons and Z^0 bosons (unaffected by the presence of a QCD medium). These studies are crucial to address the flavour dependence of the parton energy loss and will be the main focus of ATLAS and CMS, which have unique high-p_T and triggering capabilities. ALICE will complement them in the low-momentum region, and carry out measurements the flavour dependence of medium-modified fragmentation functions using light flavour, strange and charm hadrons reconstructed within jets.

Low-mass dileptons and thermal photons: these observables are sensitive to the initial temperature and the equation of state of the medium, as well as to the chiral nature of the phase transition. The study will be carried out by ALICE, which will strengthen its unique very efficient electron and muon reconstruction capabilities down to almost zero p_T, as well as the read-out capabilities for recording a very high statistics minimum-bias sample.

Figures 21 presents the projected performance in PbPb collisions (L_{int} = 10/nb) for two benchmark measurements. The left-hand panel of shows the projected ALICE performance for the measurement of the nuclear modification factors of charm (via $D^0 \rightarrow K^- \pi^+$) and beauty (via non-prompt $J/\psi \rightarrow e^+ e^-$). The precision of the measurement and the broad p_T coverage will allow for a detailed characterization of the quark mass dependence of parton energy loss and, in conjunction with the elliptic ow measurements, of the diffusion coefficients for *c* and *b* quarks in the medium. The right-hand panel of Fig. 21 shows the projected ALICE performance on the ratio of the nuclear modification factors of J/ψ

and ψ', integrated from $p_T = 0$, as a function of PbPb collision centrality. The measurement will provide discrimination between two models that describe the production of charmonium in terms of the competing effects of dissociation and regeneration in a deconfined medium.

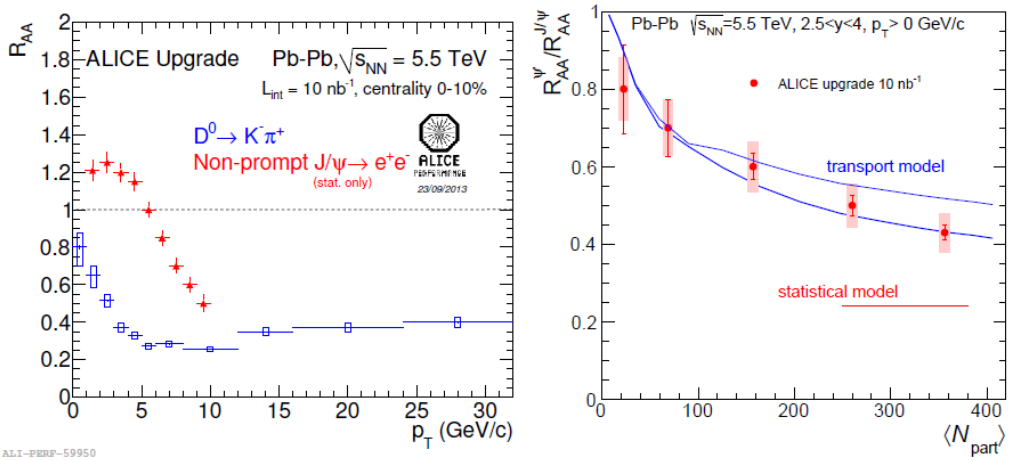

Figure 21: Left: ALICE performance on the nuclear modification factors of charm and beauty. Right: ALICE performance on the ratio of the nuclear modification factors of J/ψ and ψ'. See text for details.

5.2. The ALICE upgrade

The ALICE detector consists of a variety of detector systems for measuring hadrons, leptons and photons. It is designed to perform measurements of high-energy nucleus-nucleus collisions in order to study quark matter (QCD matter) under extreme conditions. A schematic view of the ALICE detector is shown in Fig. 22. The experiment consists of a central barrel ($|\eta| < 0.9$), placed inside a large solenoidal magnet providing a 0.5 T field, and a muon spectrometer at forward rapidity ($-4 < \eta < -2.5$).

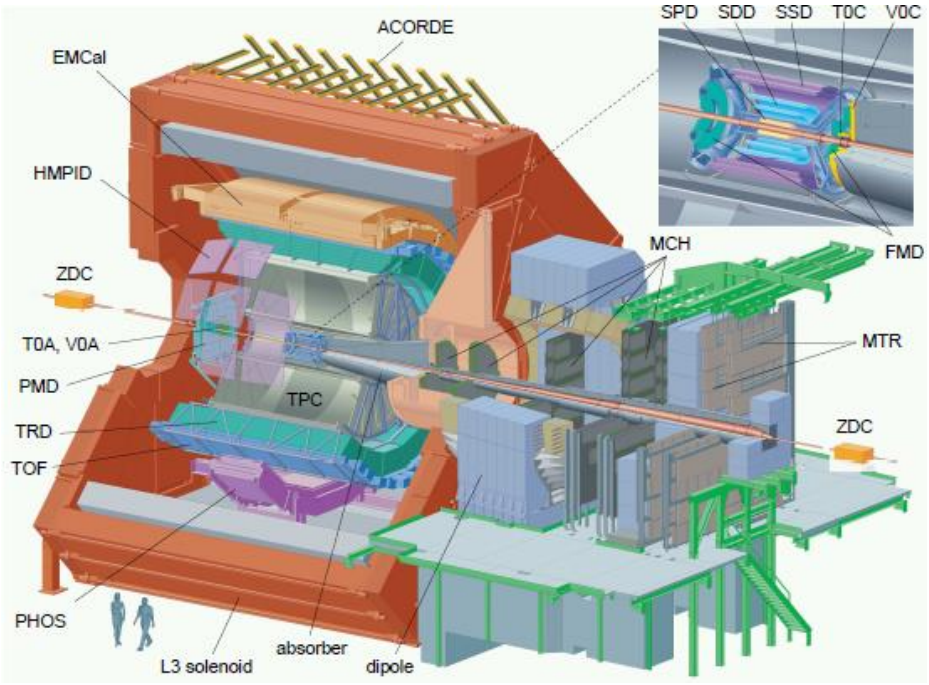

Figure 22: Schematic view of the ALICE detector. The central-barrel detectors – Inner Tracking System (ITS), Time Projection Chamber (TPC), Transition Radiation Detector (TRD), Time Of Flight (TOF), Photon Spectrometer (PHOS), Electromagnetic Calorimeter (EMCal), and High Momentum Particle Identification Detector (HMPID) – are embedded in a solenoid magnet. The cosmic-ray trigger detector ACORDE is positioned on top of the magnet. The ALICE forward detectors include the preshower/gas-counter Photon Multiplicity Detector (PMD), the silicon Forward Multiplicity Detector (FMD), quartz Cherenkov detector T0 and plastic scintillator detector V0 and the Zero Degree Calorimeter (ZDC).

At central rapidity the R_{AA} and the v_2 of D mesons in PbPb collisions were measured from Run I data, down to p_T = 1 and 2 GeV/c, respectively. Very precise measurements down to p_T = 0 for D mesons, including also D_s, represent one of the primary goals of the future ALICE heavy flavour programme. Another important target is the exclusive Λ_c baryon reconstruction, which is the most challenging heavy flavour measurement, because the small mean proper decay length ($c\tau$ = 59 μm) prevents an effective background rejection based on the decay topology selection. A sizable part of the heavy flavour programme at central rapidity includes the reconstruction of beauty hadrons, both via inclusive and exclusive decay channels. Another ambitious goal is the full reconstruction of the Λ_b baryon that will open the possibility to investigate the beauty baryon sector in PbPb collisions.
At forward rapidity the existing Muon Spectrometer provided interesting results from Run I data. However it has an important limitation since no track constraints in the region of the primary vertex are available. This is mainly due to the large distance of the tracking stations from the primary vertex in combination with the multiple scattering induced on the muon tracks by the frontal absorber. Therefore the details of the vertex region are completely smeared out. The installation of a high-position-resolution tracker would improve the resolution of muon tracks in the primary vertex region, allowing to disentangle open charm and beauty contribution to muon production and enabling the separation between prompt and displaced J/ψ mesons. Furthermore it would help in rejecting background muons coming from semi-muonic decays of pions and kaons, which represent a large background source both in single muon and dimuon analyses.

5.2.1 ALICE upgrade strategy

In order to fully exploit the scientific potential of the Heavy Ion part of the LHC upgrade in LS2 (2019-2020), the ALICE collaboration is undertaking a major initiative to extend its physics program. The improvement of the ALICE detector will enable detailed and quantitative characterization of the high density, high temperature phase of strongly interacting matter, together with the exploration of new phenomena in QCD. The ALICE upgrade plans foreseen for the LS2 are discussed in the ALICE Upgrade Letter of Intent [16]. The primary goal of ALICE is to perform high precision measurements of rare probes down to low transverse momentum.
To achieve the goals described above, high statistics and high precision measurements are necessary. Many of these measurements will involve complex probes at low transverse momentum, where traditional methods for triggering will not be applicable. Therefore, the ALICE collaboration is planning to upgrade the current detector by enhancing its low-momentum vertexing and tracking capability, and allowing data taking at substantially higher rates.
After the second long shutdown in 2018, the LHC will progressively increase its luminosity with lead beams eventually reaching an interaction rate of about 50 kHz, or luminosities of 6 x 10^{27}/cm^2/s. In the proposed upgrade, the ALICE Offline-Online computing system is upgraded (the “O2” project, see Ref. 17] for details), which allows to record PbPb collisions at the interaction rate of 50 kHz. The ALICE upgrade physics reach assumes an integrated luminosity of 10/nb (corresponding to about 10^{11} interactions). This is the minimum needed to address the proposed physics program with focus on rare probes both at low and high transverse momenta as well as on the multi-dimensional analysis of such probes such as centrality, event plane and multi-particle correlations. A special low-magnetic-field run with 3/nb of integrated luminosity for low-p_T di-electron study is as well planned.

5.2.2 ALICE detector upgrade

The planned upgrades will preserve the current particle identification capability while enhancing the vertex detectors, triggering and tracking capabilities. They include:

Inner Tracking system ITS: The new ITS, described in the ITS TDR [18] and sketched in Fig. 23, will improve the impact parameter resolution (by a factor 3 and 6 in r' and z, direction respectively), the tracking efficiency, the transverse momentum resolution and the readout capabilities. The

improvement of the impact parameter resolution will be realized by placing the first ITS layer at 22.4 mm from the beam line (present value: 39 mm) as well as by reducing the total material budget per layer: the usage of Monolithic Active Pixel Sensors (MAPS) and the optimization of front-end electronics can reduce it from the present value of 1.14% X_0 to 0.3% X_0 for the three innermost layers. Both the impact parameter at high p_T and the transverse momentum resolution will be improved by increasing the detector segmentation: all layers will be segmented in pixels with dimensions 30 x 30 μm^2 (to be compared with 50 x 425 μm^2 for the present ITS). Finally the tracking efficiency and the p_T resolution will be further improved by increasing the number of detector layers from six to seven.

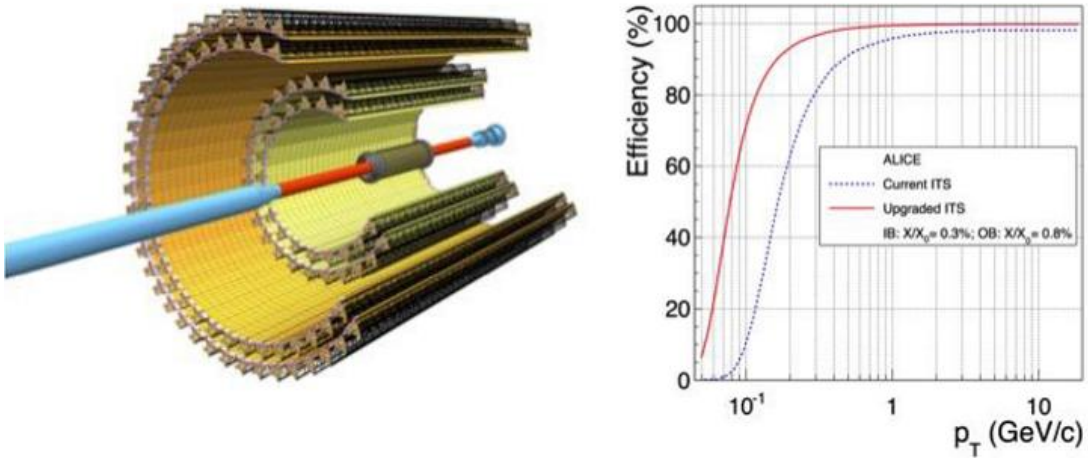

Figure 23: Left: Schematic view of the ITS upgrade, showing the inner middle and outer layers and the beampipe. Right: Simulated efficiency of the ITS upgrade as function of transverse momentum p_T.

Muon Forward Tracker MFT: The MFT detector layout and the expected physics performance are described in the ALICE MFT TDR [19]. The MFT detector will surround the vacuum beam-pipe and will be positioned inside the ITS outer barrel (four outermost ITS layers), in front of the hadron absorber of the Muon Spectrometer. It will consist of 5 layers (each one made by two half-disks) of silicon pixel sensors sharing the same pixel technology as the new ITS. Each layer will be equipped by two detection planes and the corresponding total material budget is expected to be 0.6% X_0. The muon tracks reconstructed in the muon spectrometer will be extrapolated through the absorber and matched with track segments reconstructed in the MFT planes, enabling the precise determination of the muon production vertex. Performance studies show that the offset resolution is better than 100 µm above 1 GeV/c, which is enough to perform a reliable separation of muons from *c*- or *b*-hadron decays.

Time-Projection Chamber (TPC): Within the current ALICE apparatus, the TPC with its long drift time is limiting the rate capabilities. In order to conduct the envisaged physics program with optimum precision, exploiting the full LHC luminosity, the TPC will be upgraded, as discussed in Ref. [20]. This upgrade is intended primarily to overcome the rate limitation of the present system, which arises from the gated operation of the MWPC-based readout chambers. These readout chambers are operated with an active bipolar Gating Grid (GG), which, in the presence of a trigger, switches to transparent mode to allow the ionization electrons to pass into the amplification region. After the maximum drift time of ~100 µs the GG wires are biased with an alternating voltage that renders the grid opaque to electrons and ions. This protects the amplification region against unwanted ionization from the drift region, and prevents back-drifting ions from the amplification region to enter the drift volume. Due to the low mobility of ions, efficient ion blocking requires the GG to remain closed for ~180 µs after the end of the event readout. This gating scheme leads to an intrinsic dead time of the TPC system of ~ 280 µs, implying a principal rate limitation of readout of the TPC to about 3.5 kHz and for ALICE of ~ 300 Hz for central PbPb collisions. Operation of the TPC at the 50 kHz required for the ALICE detector readout after the LHC upgrade cannot be accomplished with the current ion-gating scheme. The TPC upgrade to 50 kHz readout rate will preserve the current tracking benchmarks.

6. Challenges and developments in detector technologies, electronics and computing

The overall strategies of the four experiments remain broadly those described in the previous sections. This part of the report will focus on new developments detector research and development, electronics, and trigger and computing requirements. Details can be found in Refs. [4] and 5].

6.1 Solid State tracking devices

Tracking detectors play a crucial role in all four LHC experiments, contributing to the identification and reconstruction of particles emerging from the collisions, especially allowing the reconstruction of short-lived particles such as charm and beauty mesons and tau leptons. To preserve these capabilities during the higher luminosity phases, all four tracking systems need to be upgraded. Technical solutions for ALICE, LHCb and the outer radius (strips/strixel) of ATLAS and CMS have been established and R&D efforts are in advanced stages, while R&D for the pixel detectors is still intensive with several solutions on the horizon. The following table gives an overview of the current options for all HL-LHC tracker sensor technologies.

	Strips/Strixel baseline / options	**Pixel outer layers baseline / options**	**Pixel inner layers baseline / options**	**Special**
ALICE	MAPS (Monolithic Active Pixels)			
ATLAS	**n-in-p planar** FZ 300µm thick AC-coupled and/or HV/HR-CMOS	**n-in-p/n planar** and/or HV/HR-CMOS	**n-in-n planar** 100-200µm active thickness and/or HV/HR-CMOS and/or **3D** and/or diamond	
CMS	**n-in-p planar** FZ 200µm *active* thickness AC- and DC-coupled and/or MCz (pref) and/or 300µm	**n-in-p planar** 100-200µm active thickness	**n-in-p planar** 100-200µm active thickness and/or **3D** sensors	**HGCAL** p-in-n planar DC-coupled large PAD sensors 100-300µm active thickness (deep diffused) or n-in-p (also deep diffused)
LHCb	UT **planar n-in-p** or p-in-n	VELO **planar n-in-p** or n-in-n		

Monolithic active pixel sensors (MAPS) are used in the ALICE upgrade, but until recently did not seem radiation tolerant enough for use in ATLAS or CMS. This improved when processes referred as high-voltage (HV) and high-resistivity substrate (HR) allowed for drift-based rather than diffusion-based charge collection. Potential improvements with respect to the passive hybrid sensor baselines are cost reduction, improved resolution and material minimisation. In spite of the tight timescale until production start, the ATLAS collaboration has decided to explore a variety of processes as candidates for both strip and pixel sensors.

Optimisation of the innermost pixel sensors provides an area with further opportunities to exploit synergies between experiments. LHCb is fairly advanced, needing to have a detector ready by LS2. A variant of the MEDIPIX chip, the VELOPIX, will be used with an n-in-p or n-in-n 55x55µm cell sensor technology while reading the whole detector at 40MHz. For ATLAS and CMS, the current technology options under study for the inner pixel sensors are diamond, planar silicon or 3D silicon sensors, where trapping will be the largest challenge. The outer pixels layers could be equipped using planar silicon technology.

6.1.1 Electronics for pixel detectors

Electronics for the future pixel system pose new and so far still unaddressed issues. Radiation tolerance of the proposed 65nm architecture has still to be demonstrated; first results are encouraging, but also point to potential issues. The RD53 collaboration here is key to success. Bump bonding should be feasible in industry with a common pixel chip cell of 50 x 50µm^2 serving 50 x 50µm^2 or 25 x 100µm^2 sensor cells. Buffering (latency) and high read-out rate are definitely challenging. Buffering and logic will be implemented locally (clusters of pixel cells). The chips will be more and more digital-like with isolated islands of analogue circuits. A good balance of the read-out capability and the necessary services (~material budget) has to be sought, and data compression is an R&D topic. Targeted R&D efforts on lightweight and high data transfer cables should be strengthened. This is particularly true for the development of electrical links driving the signals from the pixel chips to the optical transmitter placed further out in the tracking volume. Single event effects for the control parts have to be taken into account although experts agree that a triple redundancy is not necessary for the read-out out cells per se and solutions in 65nm exist. Another very important aspect to minimise the tracker material, is the development of pixel electronics powering (multi-stage DC-DC or serial powering). This is motivated by the increase in power consumption due to the larger area of the detectors and the much larger number of channels.

6.1.2 Mechanics and Cooling for tracking detectors

Silicon trackers (pixels and strips) are the detectors where the tensions from diverging requirements are strongest: low temperature; large thermal power; high stability; low material budget; use of state-of-the-art technologies; long-term reliability. For this reason, this section essentially focuses on engineering issues related to silicon tracking detectors.

Lightweight Structures: Based on the experience of the present LHC detectors, it looks indeed mandatory to tackle the issues of cooling and mechanics together at the very early stages of design. No matter which cooling configuration is chosen for the next generation of detectors (with pipes, micro-channels, or even air cooling), the design will need to cope with the on-detector cooling system as part of the structure. Moreover, in tracking detectors this feature requires particular care in the selection of materials, in order not to compromise the material budget. To achieve structural and thermal designs that are optimized, the known limits of the presently used carbon fibre technology need to be pushed and new materials like diamond, carbon nanotubes and graphene need to be carefully evaluated. Advanced production technologies, like additive manufacturing and micro-fabrication, need to be considered as concrete alternatives to standard processes.

Cooling: For the next generation of detector cooling systems, the common trend is to further lower the operating temperature with coolants down to -40oC. This goes together with the need to reduce the radiation length of the thermo-mechanical structures. A standardization of the cooling systems turned out to be a very effective solution among collaborating groups from different experiments. Over the past few years, this has led to a baseline cooling technology for the HL-LHC detectors based on evaporative CO2 systems. ATLAS IBL, CMS Phase-I Pixel, LHCb Velo and UT are or will be cooled by

means of this technology. With the present design this covers cooling power ranges up to 15 kW with the lowest achievable temperature at the detector evaporators of -40°C.

CO_2 cooling has several advantages with respect to the previous evaporative system based on fluorocarbons:

- The latent heat is significantly higher and lower flow rates are required. The diameter of the boiling channel can be significantly reduced while the impact of the high evaporation pressure is mitigated. As a result, small pipe diameters with thin wall thickness have a direct beneficial impact on the overall detector system radiation length.
- Unlike fluorocarbons, CO_2 has no environmental restriction and its cost is significantly lower.

The system that has been successfully developed in the framework of the CO_2 cooling is the so-called 2PACL: 2-Phase Accumulator Controlled Loop. This system does not require compressors in the vapour phase and pumps on the liquid side to generate the flow. This solution avoids the complications related to the oil-free compressors that would have been required in a standard system. The common effort on the 2-PACL CO_2 cooling systems has developed and produced reliable cooling plants to be used as laboratory facilities or serving the actual LHC detectors. The more challenging requirements for the next detector generation necessitate further developments. In particular the cooling power of the units must be scaled up by a factor of 2 (or more) with respect to what has been achieved today. The process will not be as smooth as might be hoped. Increasing the unit power from the actual 15kW to 30-45kW implies that the technological limits of some of the key components for the 2-PACL system will be reached.

New and interesting solutions have been developed on the evaporator side – i.e. on the local detector structures. They are based on the idea that the coolant evaporates in the part that generates the heat. This is the front-end electronics generally located in the proximity of the sensors. The micro-channel cooling technique foresees to cut tiny channels on a substrate placed right underneath the chips requiring cooling. The coolant (CO_2, fluorocarbons or another) evaporates in the immediate vicinity of the volume where the heat is generated. The temperature build-up becomes very low and the overall thermal figure of merit is excellent. The technology is mature. This solution has been adopted for the LHCb VELO and NA62. Other experiments, for example ALICE, have chosen it as a back-up option.

6.2 Scintillator-based detector developments

Scintillator-based detectors are planned for use in both tracking and calorimeter systems at the HL-LHC. In LHCb an upgrade to the tracking system based on scintillating fibres is moving into construction. ATLAS and CMS are evaluating the performance of their existing calorimeters and, in the case of CMS, investigating new scintillator-based calorimeter systems for future operations at the HL-LHC. A brief summary of progress in two areas is shown here: radiation damage effects to calorimeters and the implications for calorimeter performance at the HL-LHC; the use of small diameter scintillating fibres in a large area tracking system for the LHCb upgrade.

6.2.1 Scintillator-based calorimetry

Progress in understanding the current performance of scintillator calorimeters and the expected one for the calorimeter systems proposed for use in the HL-LHC environment is important. Particularly, the CMS electromagnetic and hadronic calorimeters in the end-cap regions will need to be replaced due to radiation damage. Therefore, vigorous R&D to identify suitable radiation-tolerant technologies is continuing. For plastic scintillator, the effect of radiation damage on the sampling systems which form the hadronic calorimeters in ATLAS and CMS has been investigated, and the experiments have detailed predictions for absorbed dose and expected light losses in their calorimeters based on gamma and hadron irradiations. The degradation is monitored by calibration systems based on radioactive

sources that allow corrections to be implemented. These calibrations are taken at a frequency of 1 per month to 1 per few months and therefore provide information largely on permanent damage.

At the end of Run 1, ATLAS measured a radiation-induced signal loss of ~2% for an absorbed dose of 2.2 krad in the most irradiated cell. CMS measured a similar signal loss of ~5% for an absorbed dose of 3 krad in the barrel hadron calorimeter. A major difference of the two experiments is the pseudo-rapidity coverage and geometry of the scintillator calorimeter systems. ATLAS extends to $|\eta|=1.6$, while CMS extends to $|\eta|=2.8$, and the inner radius of the hadron calorimeter in ATLAS is 2.2 m, while for CMS the inner radius of the scintillator tile closest to the beampipe is 0.40 m. Consequently the maximum doses seen in the ATLAS hadron Tile calorimeter are ~100 times smaller than those in the CMS hadron scintillator calorimeter. For CMS, the absorbed dose in the highest η cells is 0.1- 0.2 Mrad for the 25/fb of delivered luminosity in Run I. The cells in this region showed a 30% loss of signal, about three times higher than predicted. After 3000/fb at the HL-LHC, the highest dose in the ATLAS Tile Calorimeter is expected to be 0.2 - 0.3 Mrad. Although the measured loss of signal for this dose in CMS is larger than the ATLAS expectation (30% measured by CMS compared to 15% expected by ATLAS), the light output of the ATLAS Tile Calorimeter is sufficient. Therefore even for this increased level of damage, there should be no impact on the calorimeter performance through HL-LHC operation.

6.2.2 Scintillating fibre tracking

Scintillating plastic fibres (SciFi) as active elements in tracking systems have been exploited for more than 30 years. They allow building intrinsically fast and particularly low mass detectors with a high degree of geometrical adaptability. On the other hand, the achievable spatial resolution is correlated with the fibre diameter and hence with the light yield, unless one conceives staggered multi-layer fibre arrangements which come at a cost in terms of number of read-out channels and material budget. A further limitation is the moderate radiation hardness of plastic scintillators which prevent their use in very harsh environments. The dramatic evolution of photo-detection technology, currently culminating with the SiPM devices, has revived the interest in the SciFi technology and opens up new fields of application. The intrinsic properties of the SiPM, in particular the combination of high sensitivity, high gain and fast response, implemented in a solidstate sensor of sub-mm^2 size, allow designing large-scale high-resolution SciFi detectors that can be read out at LHC speeds.

LHCb is developing a large planar SciFi tracker, consisting of blue emitting scintillating plastic fibres of 250 µm diameter, 2.5 m long and mirror coated at one end. The scintillation light exiting at the other end is detected by linear arrays of SiPM detectors (128 channels of 0.25 x 1.6 mm^2 size). The hit efficiency is directly linked to the amplitude of the signals and the minimum threshold at which the photodetector can be operated. In a harsh radiation environment, as expected at LHCb, the operation and the achievable performance of the detector are fully governed by radiation related effects. The ionising dose (up to 35 kGy in the inner region close to the LHCb beampipe) degrades the transparency of the scintillating fibre and hence the amplitude of the detectable signal. The SiPMs, located more than 2.5 m above and below the beampipe, are exposed only to small ionizing doses, however they suffer from a neutron fluence of up to $1.2\cdot10^{12}$ cm^{-2} (1 MeV equivalent). Proportional to the neutron fluence, the leakage current (or, equivalently, the dark noise rate) of the SiPMs rises to values which de facto makes them unusable. 'Normal' operation can be restored by cooling the SiPMs, which suppresses the noise rate by a factor of about $2^{\Delta T/10}$. The SiPMs in the LHCb SciFi Tracker are therefore foreseen to operate at -40°C.

6.3 Gaseous detector systems

Gaseous detectors are widely used at the LHC experiments, especially for the large areas needed for the muon detection. Most of these systems belong to one of the three following configurations:

- Drift tubes (DTs) employed in the muon systems of ATLAS and CMS, in the ATLAS Transition Radiation Tracker and in the LHCb Outer Tracker;

- Multi-Wire Proportional Counters used in the ATLAS and CMS Cathode Strip Chambers for tracking, in the LHCb Muon System and in the ALICE Time Projection Chamber, Transition Radiation Detector, RICH detector and Muon Tracking Chambers;
- Resistive Plate Chambers (RPCs) installed in the large Muon Systems of ATLAS, CMS and ALICE for Triggering, and in the ALICE Time Of Flight system (TOF).

An exception to this picture is the innermost region of the first station of the LHCb Muon System, where, due to the high particle rates, it was decided to install Micro-Pattern Gas Detectors (MPGDs), in this case based on Gas Electron Multiplier technology. Another impressive application is the ALICE Time Projection Chamber (TPC), which is a very performant device for heavy ion physics.

All these devices have of the order of 100k $_{to}$ 1M read-out channels and are operating with high efficiency at the LHC. Gaseous detectors have also regained territory that was occupied by other technologies, for instance RPCs are now used to replace scintillators for triggering and time of flight measurements in large area systems.

For HL-LHC operation, the development of a new generation of gaseous detectors with improved performance has been made easier thanks to proper environments where groups performing R&D on various detectors can meet and exchange ideas; an example being the RD51 collaboration in the field of MPGDs. A similar collaboration is being proposed for RPCs, in addition to the already existing biennial RPC workshops. Another common issue is the quest for new eco-friendly gas mixtures. Investigating new possible candidates which will replace $C_2H_2F_4$ (for RPCs) and CF_4 (for GEMs and Wire Chambers) will require a long R&D, since many gases and gas mixtures should be tested.

6.3.1 Development of new Resistive Plate Chambers for High Radiation Environments

The RPC is a unique gaseous detector due to the absence of any drift time and, therefore, an ideal detector for fast decisions and for very high time resolutions. Moreover, the simple structure and low material cost make it suitable for very large area applications. A new generation of RPCs is in preparation to face the requirements of the HL-LHC concerning rate capability, space and time resolution. The RPC rate capability is mainly limited by the current that can be driven by the high resistivity electrodes. It can be improved with lower resistivity and thinner electrodes, and with lower liberated charge. With lower bulk resistivity the detectors can operate at higher current.

The RPCs that ATLAS and CMS are envisaging for the Phase-II of LHC will have an overall structure similar to the present ones but with gas volumes of: thinner gaps, thinner electrodes and also, possibly, a multi-gap structure if required to achieve good detection efficiency. A RPC of 1+1 mm bi-gap, and sensitive area of 18x18 cm^2, built with HPL phenolic electrodes from residual ATLAS plates and equipped with a new front end circuit was installed at about 40 cm distance from the gamma source at the GIF facility and tested for several weeks. The rate measured at full efficiency was about 20 kHz/cm^2, which is a major improvement with respect to the RPCs presently operating in ATLAS and CMS. A similar test was carried out by CMS by modifying its standard two parallel gap structure. Each gap was split into 2 gaps of 0.8 mm thickness; the prototype, of active area 45 x 45 cm^2, was built with standard HPL and front-end electronics. It showed an efficiency plateau of ~ 1 kV with streamer probability < 2 % in the middle of the efficiency plateau and a rate capability of 3 kHz/cm^2.

6.3.2 Precision Micro-Pattern Gaseous Detectors (MPGD) for large areas

For the LHC upgrades, MPGDs are proposed for the regions exposed to the highest rates and/or where high spatial resolution is needed. Out of the many different types of MPGD available, Gas Electron Multipliers (GEM) have been proposed to be used in ALICE and CMS and exploited already in LHCb; while the Micro- Megas (MM) technology has been chosen for ATLAS.

In ATLAS, the New Small Wheels (NSW) will be equipped with both sTGC and MM detectors to offer excellent robustness under HL-LHC operating conditions. The MM detectors combine precision tracking functionality with trigger capability in a single device. In total, 512 Micro-Megas chambers, each with a surface area up to 3.1 m^2, will be built, corresponding to a total detection area of around 1200 m^2, with ~ 450 μm strip pitch and 2.1 M channels overall. The main issue to be addressed for using MM detectors in high energy experiments, like ATLAS, is sparks. Sparks or discharges lead to HV breakdown with relatively long recovery times and sometimes damage to the detectors themselves. The final approach chosen to overcome this problem is based on resistive strip layer techniques to AC couple the read-out strips. In ATLAS, MMs will be operated with the μ-TPC schema, i.e. using the arrival times of the ionized electrons to reconstruct the position of the primary ionizations and thus the particle track in the drift gap of the detector. This improves the spatial resolution, in particular for tracks incidence above 10°. ATLAS has also developed the floating-mesh production technique which successfully overcomes a number of previously encountered problems and allows an easy reopening of the detector, if required.

GEMs are characterized by spatial resolution of order 100 μm, time resolution of a few ns, and detection efficiency more than 95 % even for rates exceeding a few MHz/cm^2. In order to make GEM detectors suitable for HL-LHC and particularly for the CMS Upgrade, many technology breakthroughs have had to be achieved, for instance the production of large-area GEMs with a single-mask technique has been demonstrated. A novel spacer-less and stretching technique has also been developed that allows production of large-area triple-GEM detectors without any gluing. Furthermore using these techniques allows reducing the production time to a few hours and permits easy reopening of a chamber if necessary. In CMS, GEM detectors (double stations) have been proposed in yet un-instrumented locations in the endcaps, to cover the pseudo-rapidity range $1.5 < \eta < 2.2$, for robust tracking and triggering with improved muon momentum resolution in order to restore redundancy in the muon system. Also, an additional six-layer station is foreseen to be installed in a space of around 30 cm freed behind the new end-cap calorimeters, providing coverage up to $\eta = 3$ or more. Several test beam campaigns have now demonstrated that GEMs are suitable for these applications and long term tests corroborate earlier measurements.

6.4 Electronics

The demands on the upgraded experiments in terms of impact parameter resolution, channel count, hermeticity, tracker mass, timing resolution, trigger and data read-out rates, radiation hardness etc., will place severe constraints on the required electronics. This will necessitate the design of detector specific read-out ASICs and systems, as well as specific R&D activities on electronics in the following fields:

i) Very deep sub-micron technologies (e.g 65 nm and lower)
ii) High density, low mass interconnect and hybrid technologies
iii) Radiation hardness
iv) High reliability design and qualification
v) Efficient power distribution systems and low power design techniques
vi) Low power, high speed electrical and optical links
vii) Modular electronics standards for high speed data back-end processing

The progress on IC design and technologies, and the high-speed optical and electrical links is briefly described including a discussion on use of FPGAs in the experimental caverns.

6.4.1 IC Design and Technologies

Radiation tolerant ASICs are one of the key enabling technologies of the LHC experiments. In particular, ASICs designed for radiation tolerance in 250 nm CMOS played a major role. ASICs will continue to be key components for HL-LHC, however, a number of challenges have to be faced when

keeping up with the evolution of the technology: higher hit rates, higher radiation hardness, higher trigger rate or trigger-free operation, minimisation of material and power consumption, high dynamic range design in sub-100 nm processes, high pile-up which might require sub-ns time stamping.

From the first generation of LHC ASICs it has been learnt that the selection of a CMOS process must be based as much on its commercial viability as on the elegance of the technical solutions it offers, as this impacts yield (i.e. cost) and long term accessibility. It has also been learnt that collaboration between groups works best if based on a common technology platform and that duplication of design effort, while valuable for training purposes, is not optimal. Common foundry access through CERN covers now 250 and 130 nm CMOS processes from the former IBM foundry (now Global Foundry) as well as 130 and 65 nm CMOS processes from TSMC. Radiation qualification of the latter two is on-going. In particular RD53 is performing extensive tests of the 65 nm process at the very high radiation doses required by the pixel detectors. Some not yet understood issues are observed after about 300 Mrad. An effort for sharing designs is being put in place in the framework of RD53 for the pixel electronics development in 65 nm technology. Already a number of IP blocks are available, as well as a repository and a usage agreement between collaborating institutes. A similar effort is starting for the other technologies and shall be pursued in the coming years.

Interconnecting chips to sensors is also a key process. Although aluminium wire bonding remains the dominant means of I/O from chips, flip chip is now common on high volume consumer goods and is used in some of our applications. Through Silicon Vias (TSVs) are being used in some special applications (such as smartphone camera assemblies and DRAMs) but such processes are still difficult or impossible to access in smaller volumes. However TSV-last processing (i.e. the vias are drilled on finished wafers) starts to become viable, and has been demonstrated in the context of the Medipix collaboration.

6.4.2 Electrical and Optical Links

Optical links have been instrumental in building the LHC detectors and they will also be crucial at the HL-LHC. The LHC experiments deployed optical links to an unprecedented scale for their read-out systems. The lessons learned during the development, procurement, installation and commissioning of these systems have highlighted, among other issues, the need to increase link bandwidth (to better amortize system cost), to share R&D effort (to better use the limited resources available) and to enforce extensive and rigorous quality assurance programmes (to identify shortfalls as early as possible). The “Radiation Hard Optical Link” project was launched with the objective of developing a common and “universal” optical link for data read-out, trigger and control. A 5 Gbps radiation-hard bidirectional optical link is now available with the GBT chipset and the Versatile Link transceivers. The production phase is now launched and components for the Phase-I upgrades will be delivered in 2015.

A review of the requirements for the upgrades of the ATLAS and CMS trackers as well as the read-out of the calorimeters and muon detectors have shown the necessity of developing a lower power or a higher speed version of the link (about 10 Gbps) as well as a lower mass version of the optical transceivers. The so-called lpGBT and Versatile Link+ projects are now starting with the aim of delivering a link either running at about twice the speed of the current one with the same power budget or at the same speed with about a quarter of the current power budget. Collaborative efforts for these projects are welcome as the developments of the GBT chipset and of the Versatile Link have proven to be rather time and manpower consuming.

Very harsh radiation environments and/or stringent material budget constraints sometimes preclude the use of optical links. That is for instance the case in the inner layers of the pixel detectors. The use of high-speed electrical transmission on low mass cables can then be the only solution. Several developments (e.g. for the ALICE ITS or the LHCb Velo) are looking very promising. *Silicon photonics* is

a potential paradigm shifting technology, bringing the promise of tightly integrating optoelectronics and front-end electronics. Some components are being evaluated (in particular for their radiation hardness). An increased effort would be needed, should this technology prove promising.

6.4.3 Using FPGAs in the detector cavern

The use of high-end FPGAs in the front-end electronics of some sub-detectors (those with the lowest radiation constraints) is very attractive as one can take advantage of powerful functions such as high-speed links for increased data read-out, PLLs for clock management related to synchronization with the accelerator clock or DSP blocks for data processing.
However their behaviour in radiation environments requires special care, especially the effect of single event upsets which are different for each technology (SRAM, anti-fuse and flash memory). Several mitigation techniques have been presented but it should also be noted that characterizing a device needs major effort and that the community would benefit a lot from some coordination. So far, collaboration across different projects has been rare and mainly based on the activities of interested individuals.

6.5 Developments in Triggering, Online and Offline Computing

6.5.1 Hardware Triggers

The LHC experiments face considerable challenges to exploit future increases in luminosity. After LS2, both ALICE and LHCb will adopt a “triggerless” architecture. This shifts the burden of triggering to farms of commodity processors steered by software developed in large collaborative projects and to the personnel who provide and maintain this software. ALICE will use continuously read out triggering detectors with different latencies, busy times and technologies, differently optimized for pp, pA and AA running scenarios. LHCb will run trigger-free in order to achieve a substantial increase in physics reach, reading every bunch crossing.

Although technologies may at some point evolve sufficiently, present read-out links do not allow ATLAS and CMS to adopt “triggerless” architectures with acceptable detector power and material budgets for their tracking detectors. Therefore, at the HL-LHC, both ATLAS and CMS will retain their hardware Level 1 triggers. Three changes to these trigger systems are planned during LS3. The first is the addition of a L1 tracking trigger for the identification of tracks associated with calorimeter and muon trigger objects. The second is the utilization of finer granularity information from the calorimeter and muon trigger systems. The third is a combination of significant increases in L1 rate, L1 latency, and High-Level Trigger (HLT) output rate. All three changes are required in order to realize the physics potential of ATLAS and CMS at the HL-LHC.

The ATLAS experiment will divide its L1 trigger into two stages. The first stage is a L0 trigger with a rate of 1 MHz and latency of 6 μs that will use more fine-grained calorimeter and muon information to produce seeds for a regional read-out of the tracker. The second stage L1 trigger will use this information to further reduce the rate to around 400 kHz with a total L0 and L1 latency of 30 μs. The output of the L1 Trigger will be processed by the HLT with an output to storage rate of 5 to 10 kHz. The CMS L1 trigger will retain its present architecture but its latency will increase to 12.5 μs with an output range of 500 to 750 kHz for pileup ranging between 140 and 200. CMS will use an un-seeded L1 Track trigger at 40 MHz along with finer granularity calorimeter and muon triggers. The CMS HLT output rate to storage will range between 5 to 7.5 kHz for pile-up ranging between 140 and 200.

6.5.2 DAQ and Software Triggers

The LHC beyond Run I foresees a steady increase in the fraction of collision data which is sent off-detector for processing by so-called “software triggers”, meaning any trigger stage or algorithm that is executed on commodity processors. Typically these have been CPUs, however there is an increasing

amount of R&D into massively parallel GPU and FPGA “co-processors” to aid CPU farms with those tasks that can be naturally parallelized. It is important to note that even within CPUs, the technological trend is towards more cores and by the time of Run 4 a typical CPU may well have as many cores as one of today's smaller GPUs. For this reason, it is necessary to significantly rethink almost all aspects of event reconstruction and selection in order to fully exploit the power of the data processors anticipated for the HL-LHC era, a point discussed more fully below.

All collaborations assume a steady growth in the computing power available per CHF of between 25% and 35% per annum as part of what is needed to cope with the higher instantaneous luminosities and more complex events of the HL-LHC era. In addition to this, it will be necessary to find another factor of between two and five in performance. One increasingly important strategy will be to extend the latency of software triggers to fill as much of the machine idle time as possible by using massively parallel local storage buffers composed of hard-disks attached to the individual processing nodes of the software trigger farms. LHCb is testing such a system during Run 2. Their software trigger will be split into two stages, and events buffered between the two in such a way as to keep the farm processors fully utilized between fills. Such approaches, if successful, may allow the doubling of online processing power per CHF in the HL-LHC era.

Data rates of around 40Tb/s going into the ATLAS, CMS, and LHCb software triggers imply an overall volume of around 60 exabytes of data to be processed per year of data taking, a volume comparable to the largest commercial data processing tasks. Such data rates will be especially challenging because the events will be packed with interesting physics that these state-of-the-art detectors should be able to study. For example, a bunch crossing at ATLAS and CMS during Run 4 will contain on average one bottom pair and twenty charm pairs, while the rate of fully reconstructed signal for certain key *CP*-violating observables will exceed 2 kHz at LHCb. In the case of ALICE, every single bunch crossing (50 kHz in Pb-Pb and 200 kHz in p-Pb collisions) is considered interesting and the role of the trigger system is to compress each bunch crossing by a factor 100, rather than rejecting any events. In such a signal-dominated environment it will become increasingly important to shift more of the final analysis burden from the offline processing to the software trigger, and to consider new data processing paradigms such as analysis using trigger-level objects, or saving only part of each event through suppression of raw data which is associated with pile-up vertices. While ATLAS and CMS aim to write out between 5 and 10 kHz of events for offline analysis, and LHCb between 20 and 100 kHz, these “events” will most likely no longer be the traditional full raw detector output, but rather a heterogeneous mixture of full events, trigger-level analysis objects, data mining events for long-term archival (“parking”) and other compressed data formats. In addition, as the software triggers will increasingly discriminate between different signals rather than between signal and backgrounds, it may also be important to perform the detector alignment and calibration in real time, as well as developing multivariate analysis methods which are safe for online use.

6.5.3 Software and Computing

Trends in hardware evolution have continued to demonstrate the validity of Moore's Law, viz. the density of transistors on CPUs doubles roughly every 24 months. However, whether this scaling holds, even for the next decade, remains a subject of intense research and a slow down to a doubling every 36 months is entirely possible. For the HL-LHC timescale this leaves some uncertainty over the “raw” computing power that might be available. The principle driver for computing hardware is now energy consumption, with the figure of merit being nanoJoule/instruction. Even if the more optimistic predictions are realised, it is already clear that modern computing hardware is becoming increasingly hard to exploit effectively. One of the most difficult areas to tackle, given the large amounts of legacy code in the experiments, is that of data layout. The performance gap between memory and CPU has been increasing and hundreds of cycles can be wasted while data and instructions are fetched from main memory. Here a paradigm shift from *object oriented design* to *data oriented design* will allow

the knowledge of other communities to be applied to HEP. This re design of in memory event storage and algorithms will be a fundamental part of preparing for HL-LHC and will be essential to move computations efficiently from CPUs to accelerators or FPGAs. The kernel code for core algorithms will need to be portable to many platforms as the era of an x86_64 mono-culture is almost certainly over.

In exploiting multi-core architectures the LHC experiments have now made significant progress. CMS have now demonstrated a multi-threaded version of their framework that scales well and saves huge amounts of memory. ATLAS and LHCb have collaborated on the GaudiHive, which is being developed aiming at Run 3 and has also shown good scaling, albeit in limited reconstruction cases. ALICE have an ambitious plan to develop a new framework, O^2, which unifies online and offline processing.

For costly algorithmic code, which must be adapted to make best use of parallelism and features like Single Instruction Multiple Data (SIMD), there are practical demonstrations that show significant progress. e.g., the Geant V project has successfully parallelised particle transport as well as implemented vectorized code for common geometry operations. Track triggers remain a challenge to simulate, as reproducing the logic of an associative memory on CPU devices is extremely slow and inefficient. Fast simulation strategies will be important to develop to keep up with event complexity and rate at HL-LHC. For tracking, which dominates the reconstruction time at high pile-up, many parallel algorithms are available. However, realistic studies of likely physics performance are needed to balance cost of serial approaches (which can better reduce combinatorics) and parallelism (which can utilise more cores); the goal is overall improved throughput with robust physics performance. These same goals apply equally to other areas.

Once data have been reconstructed, offline computing will have to cope with roughly an order of magnitude larger raw data volume in the HL-LHC era. While the cost of archival tape storage is expected to be similar to today, disk storage at sites storing derived data copies, caches, etc., may fall short by a factor of 2-3, based on current extrapolations. As for online software triggers, the cost of CPU is expected to be 2-5 times more than flat budgets. Any shortfalls will need to be primarily addressed by better use of computing resources. In contrast, networking has seen a steady exponential growth and expected technology developments will likely see this continue, which should provide ample network capacity for HL-LHC. There also exist possibilities to use networks more extensively to offset disk requirements with fewer disk resident copies and more remote access to data to feed CPUs at different sites.

7. Conclusions

A summary of the physics motivation, the conceptual designs and the expected performance of the upgrades of the four major experiments, ATLAS, CMS, LHCb and ALICE has been given, together with the plans to develop the appropriate experimental techniques and a brief overview of the accelerator upgrade.

A central component of the HL-LHC program is to perform precision measurements of the properties of the 125 GeV Higgs boson and compare these to the predictions of the SM. The ATLAS and CMS experiments concluded that with an integrated luminosity of 3000/fb the HL-LHC is a very capable precision Higgs physics machine. The studies performed also demonstrate that HL-LHC is at the same time a unique discovery machine. In addition to being sensitive to BSM physics via deviations from the SM in the Higgs sector, including the possibility of additional Higgs bosons, with HL-LHC, ATLAS and CMS will continue the direct search for other new particles that could shed light on one or more of the open questions in HEP and cosmology such as the stabilisation of the Higgs mass or the nature of dark matter. ATLAS and CMS performed studies that illustrate the importance of the large dataset that HL-LHC will provide in making such a discovery in cases where the new physics is produced with a small cross section, small visible branching fraction, or experimentally challenging kinematics.

The HL-LHC also provides exciting discovery potential through precision studies of the flavour sector. In particular, studies from LHCb demonstrate that it will be the leading experiment for a wide range of important observables concerning rare decays and *CP* violation in charm and beauty hadrons. This capability is complemented by sensitivity from ATLAS and CMS in particular channels triggered by dimuon signatures. Lastly, in addition to high luminosity proton operation, the HL-LHC will provide a substantial integrated luminosity of heavy ion collisions. The impact that a dataset of 10/nb of PbPb collisions will have on the precision of a variety of physics observables that will be used to further our understanding of the quark-gluon plasma.

Acknowledgements

Most of the material shown in the lectures and referred to in these proceedings has been shown at the two ECFA HL-LHC workshops in Aix-les-Bains, France October 1-3, 2013, and on October 21-23, 2014 and the RLIUP workshop, Archamps, France, October 29-21, 2013. The key points of these workshops have been summarized in Refs. [4+5], and the upgrade plans of the experiments in documents submitted to the Large Hadron Collider Committee (LHCC), to which references are made in these proceedings. Sincere thanks to the many colleagues who prepared the material which could be used in the lectures and this report.

References

[1] ATLAS Collaboration, *"Observation of a new particle in the search for the Standard Model Higgs boson with the ATLAS detector at the LHC"*, Phys. Lett. B **716** (2012) 1

[2] CMS Collaboration, *"Observation of a new boson at a mass of 125 GeV with the CMS experiment at the LHC"*, Phys. Lett. B **716** (2012) 30

[3] CMS and LHCb collaborations, *"Observation of the rare $B_s^0 \rightarrow \mu^+\mu^-$ decay from the combined analysis of CMS and LHCb data",* Nature 522, 68–72, June 2015

[4] D. Abbaneo et al. *"ECFA High Luminosity LHC Experiments Workshop: Physics and Technology Challenges", (ECFA/14/284), https://cds.cern.ch/record/1631032.* November 2013

[5] M. Abbrecia et al. *"ECFA High Luminosity LHC Experiments Workshop: Physics and Technology Developments", (ECFA/15/289), https://cds.cern.ch/record/1983664.* January 2015

[6] D. Brünnig and L. Rossi (Eds.) *"The High Luminosity Large Hadron Collider"*, Advanced Series on Directions in High Energy Physics – Vol. 24, ISSN 1793-1339, World Scientific, (2015).

[7] ATLAS Collaboration, "*Letter of Intent for the Phase-I Upgrade of the ATLAS Experiment",* CERN-LHCC-2011-012, LHCC-I-020, (2011).

[8] ATLAS Collaboration, "*Letter of Intent for the Phase-II Upgrade of the ATLAS Experiment",* CERN-LHCC-2012-022, LHCC-I-023, (2012).

[9] CMS collaboration, *"Technical Proposal for the Phase-II upgrade of the Compact Muon Solenoid"* CERN-LHCC-2015-010, LHCC-P-008, (2015).

[10] LHCb collaboration, *"LHCb Upgrade Letter of Intent",* CERN-LHCC-2011-001, LHCb-LOI, (2011).

[11] LHCb collaboration, *"Framework TDR for the LHCb upgrade",* CERN-LHCC-2012-007, LHCb-TDR-012, (2012).

[12] LHCb collaboration, *"LHCb upgrade Trigger and Online TDR"*, CERN-LHCC-2014-016, LHCb-TDR-016, (2014).

[13] LHCb collaboration, *"LHCb upgrade Velo TDR"*, CERN-LHCC-2013-021, LHCb-TDR-013, (2013).

[14] LHCb collaboration, *"LHCb upgrade Tracker TDR",* CERN-LHCC-2014-001, LHCb-TDR-015, (2014).

[15] LHCb collaboration, *"LHCb upgrade Particle Identification TDR",* CERN-LHCC-2013-022, LHCb-TDR-014 (2013).

[16] ALICE collaboration, "*Letter of Intent for the upgrade of the ALICE Experiment",* Tech. Rep., CERN-LHCC-2012-012, LHCC-I-022 (2012).

[17] ALICE collaboration, *"Addendum of the Letter of Intent for the Upgrade of the ALICE Experiment: Upgrade of the Readout and Trigger System",* CERN-LHCC-2013-019 (2014).

[18] ALICE collaboration, *"Technical Design Report for the Upgrade of the ALICE Inner Tracking System",* CERN-LHCC-2013-024 (2013).

[19] ALICE collaboration, *"Addendum of the Letter Of Intent for the Upgrade of the ALICE Experiment: The Muon Forward Tracker",* CERN-LHCC-2013-014 (2013).

[20] ALICE collaboration, "*Upgrade of the ALICE Time Projection Chamber",* CERN-LHCC-2013-020 (2013).